

**Development of binary vector systems for
promoter assay and expression analysis of
AtMLLR genes in *Arabidopsis thaliana***

(プロモーターアッセイのためのバイナリベ
クターシステム開発とシロイヌナズナにおける
AtMLLR 遺伝子の発現解析)

SULTANA MST MOMTAZ

2020

Table of contents

Abbreviations	3
Chapter 1: Introduction	7
Chapter 2: Gateway Binary Vectors with Organelle-Targeted Fluorescent Proteins for Highly Sensitive Reporter Assay in Gene Expression Analysis of Plants.	27
Chapter 3: Expression Analysis of Genes Encoding Malectin-Like Domain (MLD)- And Leucine Rich Repeat (LRR)- Containing Proteins in <i>Arabidopsis thaliana</i>	46
Chapter 4: Proposed conclusions	54
References	57
List of publications	70
Acknowledgements	71
Summary	74

Abbreviations

aadA	: spectinomycin resistance (Spc ^r) marker used for selection in bacteria
<i>A. thaliana</i>	: <i>Arabidopsis thaliana</i>
ABRC	: Arabidopsis Biological Resource Center
ABI2	: ABSCISIC ACID INSENSITIVE
AF	: autofluorescence
AtMLLR	: <i>A. thaliana</i> malectin-like leucine repeat
AtRLP4	: <i>A. thaliana</i> receptor-like protein 4
BAK1	: BRASSINOSTEROID INSENSITIVE 1 ASSOCIATED KINASE
bar	: bialaphos resistance gene
BASTA ^r	: BASTA resistance
bp	: base pair
bom	: cis-acting element for conjugational transfer
CAZy	: Carbohydrate-Active Enzymes
CBMs	: carbohydrate-binding modules
ccdB	: negative selection marker used in bacteria
cDNA	: Complementary DNA
CO	: coat protein complex
Col-0	: Columbia ecotype
Cm ^r	: chloramphenicol resistance
CrRLK1Ls	: <i>Catharanthus roseus</i> receptor-like kinase 1-like proteins
DAD1	: DEFFECTIVE IN ANTHER: DEHISCENCE1
DALL2	: DAD1-LIKE LIPASE2
DIC	: differential interference contrast
EC	: extracellular
ECDs	: extracellular domains
<i>E. coli</i>	: <i>Echerichia coli</i> .
eJM	: extracellular juxta-membrane
EN14	: EARLY NODULIN
ER	: endoplasmic reticulum
<i>erd1</i> mutant 1	: ER retention defective mutant 1
<i>erd2</i> mutant 2	: ER retention defective mutant 2

GEF1/4/7/10	: GUANINE NUCLEOTIDE EXCHANGE FACTOR 1/4/7/10
FER	: FERONIA
GFP	: Green Fluorescent Protein
flg22	: flagellin epitope 22
FLS2	: FLAGELLIN SENSING 2
FMV	: fig mosaic virus
GPI	: glycosylphosphatidylinositol
GPT	: UDP-N-acetylglucosamine: dolichol phosphate N-acetylglucosamine-1-P transferase
HDEL	: his-asp-glu-leu
HPT	: hygromycin phosphotransferase
Hyg ^r	: hygromycin resistance
IC	: intracellular
IHF	: Integration Host Factor
IM	: inner membrane
KAT2	: 3-ketoacyl-CoA thiolase 2
KD	: kinase domain
KDEL	: lys-asp-glu-leu
Km ^r	: kanamycin resistance
LAS AF	: Leica Application Suite Advanced Fluorescence
LB	: left border
LR	: Luria broth
LRE/LLG1	: LORELEI and LORELEI-LIKE GPI-ANCHORED PROTEIN 1
RB	: right border
<i>Ler.</i>	: <i>Landsberg erecta</i>
LRR	: Leucine Rich Repeat
MAPKs	: mitogen-activated protein kinases
MLD	: malectin-like domain
MPP	: mitochondrial processing peptidase
mRNA	: messenger RNA
MS	: Murashige and Skoog
mtHsp70	: mitochondrial heat shock protein 70
Mt	: Mitochondria

NASC	: Nottingham Arabidopsis Stock Center
NLS	: nuclear localization signal
nos	: nopaline synthase
NPTII	: neomycin phosphotransferase II
ORF	: Open Reading Frame
ori	: ColE1 replication origin
PCR	: Polymerase chain reaction
pGWBs	: Gateway binary vectors
PI-PK β 1	: plastidial pyruvate kinase β subunit gene
PKA	: cAMP- dependent protein kinase A
PM	: plasma membrane
Pnos	: nopaline synthase promoter
Pro35S	: 35S promoter
p-SFKs	: phosphorylation of SFKs
PSs	: presequences
PTS	: peroxisomal targeting signal
Px	: Peroxisome
RALF1/23	: RAPID ALKALINIZATION FACTOR 1
rep	: broad host-range replication origin
RLP	: Receptor like protein
RIPK	: RESISTANCE TO PSEUDOMONAS SYRINGAE PV. MACULICOLA 1–INDUCED PROTEIN KINASE
RLKs	: receptor-like kinases
RNC	: ribosome nascent chain
ROP2/11	: RHO-GTPASE OF PLANTS 2
SAM1/2	: S-ADENOSYLMETHIONINE SYNTHASE 1 and 2
SFKs	: Src family kinases
sGFP	: synthetic GFP
SKL	: serine-lysine-leucine
SP	: Signal Peptide
SP _{spo}	: sporamin A SP
SP _{cal}	: Calreticulin SP
SP _{clv}	: CLAVATA3 SP

SRP	: signal recognition particle
Sta	: region for stability
TagRFPs	: tag red fluorescent protein
T-DNA	: transferred-DNA
TIM	: translocase of the inner membrane
TM	: transmembrane
TMD	: transmembrane domain
Tnos	: nopaline synthase terminator
Tom20	: translocase of the outer membrane 20
Tunica ^r	: tunicamycin resistance
WT	: wild type

Chapter 1

Introduction

Arabidopsis thaliana

Arabidopsis is a member of the mustard (Brassicaceae) family, which includes cultivated species such as cabbage and radish. *Arabidopsis thaliana* is an annual (rarely biennial) small flowering plant, usually growing to 20–25 cm tall[1]. *A. thaliana* is native to Europe, Asia, Africa. In tropical alpine ecosystems in Africa and perhaps South Africa it also appears to be native[2][3]. In the 17th century, it has been familiarized and accepted worldwide, including in North America[4]. *A. thaliana* keenly habituated in sandy, rocky and calcareous soils. Because of its extensive spreading in agricultural fields, railway lines, waste ground, roadside and other distressed habitation, it is usually considered as a weed.

A. thaliana has been widely considered as a model for flower development. The emerging flower has four basic structures: sepals, petals, stamens, and carpels. These structures are organized in a series of whorls: four sepals on the external whorl, followed by four petals inside this, six stamens, and a central carpel region. Researches of *A. thaliana* have provided significant perceptions with favors to the genetics of leaf morphogenesis, principally in dicotyledon-type plants[5][6]. The formation of *A.*

thaliana leaves at the base of the plant is rosette. They are relatively simple and stable and have been broken down into three stages (the initiation of the leaf primordium, the establishment of dorsiventrality, and the development of a marginal meristem are appropriate for research of leaf development).

Agronomic significance of *Arabidopsis* is not foremost, but its small genome size and effortless cultivation suggest significant advantages for basic research in genetics and molecular biology. Genome size of *A. thaliana* is ~135 Mb, and the chromosome number is haploid which is five. This is the first plant whose genome was sequenced[7]. For several plant traits, including flower development and light sensing it is broadly used as a model organism in plant biology and genetics.

A. thaliana has numerous practices for genome analysis, together with a short generation time (four to six weeks), large number of offspring, small size, and a relatively small nuclear genome (only five chromosomes $2n = 10$)[8][9][10]. These advantages stimulated the development of a scientific community that has explored the biological processes of *Arabidopsis* and has categorized several genes together with their functions.

In recent years, it has been the topic of numerous researches and it is the utmost broadly studied plant species with over 50,000 thousand of articles dealt with development and evolution of its biochemistry and molecular genetics by 2015[11]. Contributing to the study of *Arabidopsis* is a better understanding of the different biological advances not only in plants but also in animals and other organisms that have so far maintained numerous genes in all eukaryotes.

Genetic transformation of *A. thaliana* is maintained by transportation of T-DNA (transferred DNA) from *Agrobacterium tumefaciens* to the plant genome[12][13]. Categorized accessions and mutant lines of *A. thaliana* were used as experimental material in laboratory research. The most frequently used background lines are *Ler.* (Landsberg *erecta*) and Col. or Columbia. (NASC-Nottingham Arabidopsis Stock Center). Whereas other background lines such as Ws, or Wassilewskija, C24, Cvi, or Cape Verde Islands, Nossen, etc are rarely cited in the scientific literature[14]. Columbia (Col-0) ecotype is distinguished as the reference genotype due to its accessible information composed from numerous physiological, biochemical, sequencing and microarray investigation.

The *A. thaliana* gene knockout collections are the exclusive source of plant biology that were made possible by high-through transformation and the availability of whole genomic sequences. The site of T-DNA insertions has been determined for over 300,000 independent transgenic lines that are necessary for a plant to function accessible through online T-DNA databases (<http://signal.salk.edu/cgi-bin/tdnaexpress>) and complete genome microarrays that already exist in several basic statistics databases, such as TAIR (<http://www.arabidopsis.org/>) and Arabidopsis Biological Resource Center (ABRC) (<https://abrc.osu.edu/>).

GATEWAY Cloning Technology

GATEWAY Cloning Technology is a worldwide system for cloning DNA fragments-where all forms of DNA fragments can be cloned (cDNAs, genomic DNA, PCR fragments) into virtually any kind of vector (expression, sequencing, viral, plasmid). In the GATEWAY system, a sequence can be transferred into GATEWAY vector while maintaining reading frame and orientation by simply adding proteins, incubating, and

transforming *E. coli*. The Gateway cloning system makes an innovative trend in molecular biology by addressing the complications of adaptability, compatibility and efficiency of the traditional cloning approaches. So, it is a powerful novel practice that significantly enables protein expression, cloning of PCR products, and searching of gene function by swapping restriction endonucleases and ligase with site-specific recombination.

GATEWAY Cloning Technology based on the recombination reactions used by phage λ [15] that mediate the integration and excision of its DNA into *E. coli* genome[16][17]. Both organisms have precise recombination sites called *attP* (242 bp) in phage λ site with the *attB* (25 bp) site situated in the bacterial genome. The integration procedure (lysogeny) is catalyzed by two enzymes: the phage protein integrase (Int) and the bacterial protein integration host factor (IHF) (collectively referred to as "BP Clonase"). Upon integration, the recombination between *attB* (25 nt) and *attP* (243 nt) sites create *attL* (100 bp) and *attR* (168 bp) sites that flank the integrated phage λ DNA (Fig 1.1).

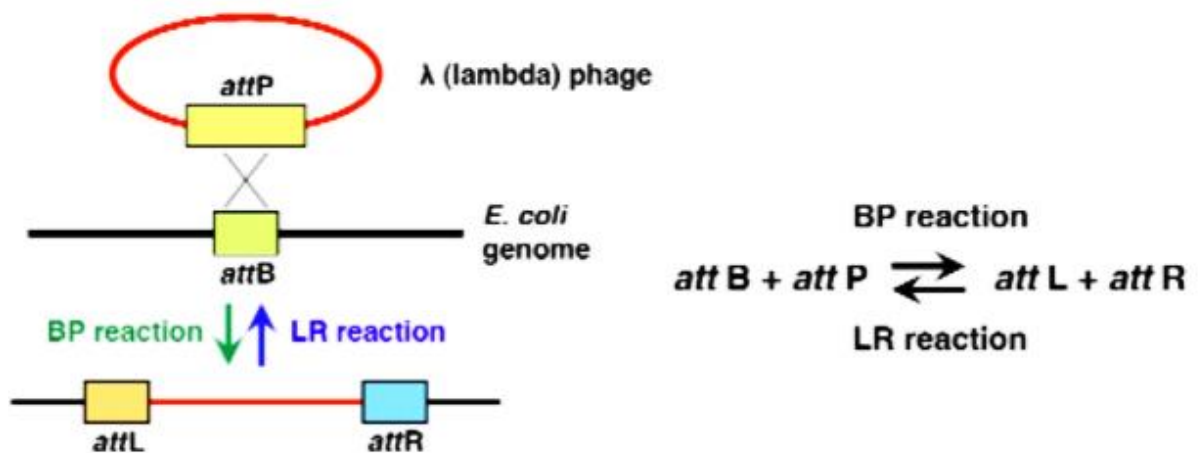


Fig. 1.1 Outline of Gateway cloning showing the site-specific recombination and the BP and LR reactions. [Cited from (Y, Tanaka, *et al.* (2012), *Genetic Engineering – Basics, New Applications and Responsibilities*)[18].

The recombination reaction is reversible reaction that requires Int, IHF, and an additional phage enzyme, excisionase (Xis) (collectively referred to as "LR Clonase"). It is an "operating system" for the immediate use of authorized clones and expression vectors between different laboratories. Once the gene sequences are transformed into entry clones,

virtually can be cloned into any type of destination vector, maintaining the reading frame and orientation, and maximizing flexibility to easily transfer DNA sequences from one expression vector to another. This greatly speeds authentication of clones, for example, in a two-hybrid screen[17][19]. For the purpose of GATEWAY cloning, the recombination reactions have been modified in several ways[17]. First, both BP and LR Clonases have been cleansed, permitting the GATEWAY reactions to occur in vitro. Second, the *att* sites have been mutated to create couples of derivatives: modification of *attB* into *attB1* and *attB2*, *attP* into *attP1* and *attP2*, *attL* into *attL1* and *attL2*, and finally *attR* into *attR1* and *attR2*. These sites were designed into recombination reactions can occur only between *attB1* and *attP1*, *attB2* and *attP2*, *attL1* and *attR1*, and *attL2* and *attR2*. The duplication of *att* sites permits two independent recombination reactions to take place in the similar molecules, one at the 5' end of the ORF to be cloned and the other at the 3' end. Third, the sequence of the *attB1* and *attB2* sites was designated into each frame which is open and therefore both N- and C terminal fusion proteins can be generated. Donor vectors transmit a cassette flanked by *attP1* and *attP2* sites (*attP1-attP2*) that are compatible for recombination with the *attB1* and *attB2* sites. Using this configuration, a PCR product containing an ORF flanked by *attB1* and *attB2* (*attB1-ORF-attB2*) can be readily recombined into a Donor vector. This will generate an Entry clone containing the ORF flanked by *attL1* and *attL2*. The *attB1* and *attB2* sequences are only 25 nucleotides long and can be added to the primers used for PCR amplification of the ORFs. Destination vectors carry a cassette flanked by *attR1* and *attR2* sites (*attR1-attR2*) that can recombine with the *attL1* and *attL2* sites of the entry clones, respectively[20] . Importantly, the 5' and the 3' ends of the ORFs recombine in a direction-dependent manner during both the BP and the LR reactions. Donor vectors with appropriate flanking *att* sites cloning with the right destination vector and LR reaction performed to yield final expression vectors (Fig 1.2)[21].

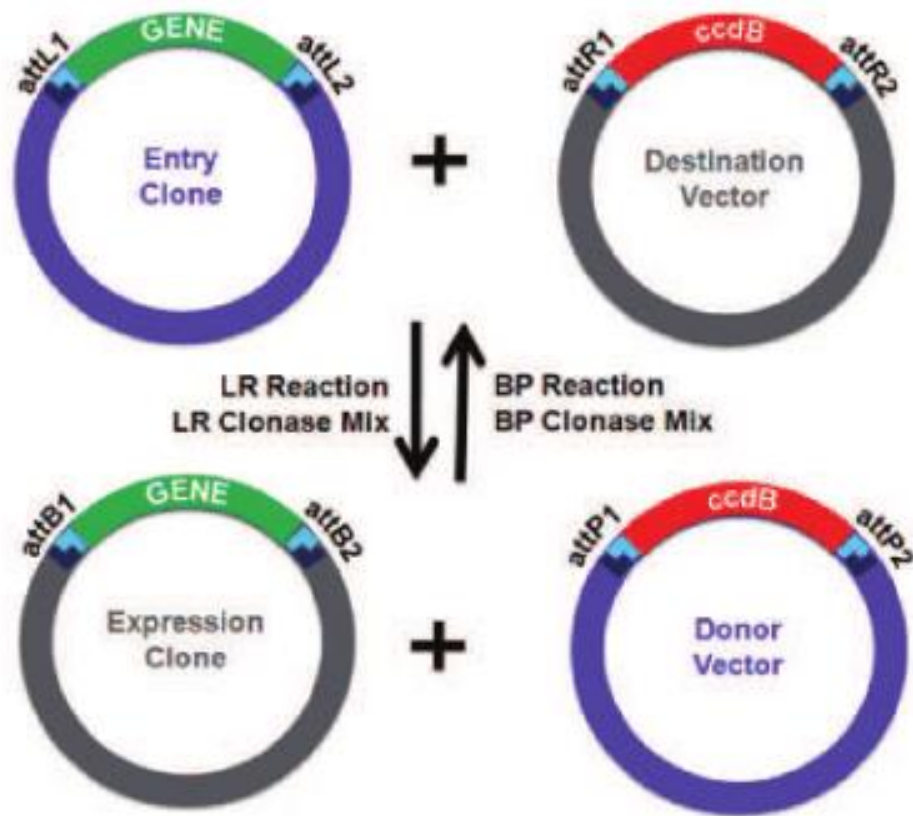


Fig. 1.2. Gateway cloning technology. [Cited from: Fontes, *et al.* (2011), *Stem Cells in Clinic and Research*, InTech] [21] .

Both cassettes of GATEWAY vectors, between the *att* sites (*attP1-attP2* and *attR1-attR2*), *ccdB* gene whose protein product interferes DNA gyrase and a chloramphenicol resistance (Cm^r) marker are advantageous for selection and maintenance of Gateway vectors. Gateway cloning has excessive benefits: it is free from the need for restriction digestion, has a simple and uniform protocol, and offers high efficiency and reliability of cloning, easy manipulation of fusion constructs, and the existence of a variety of destination vectors for many purposes. Since compatibility is a very significant resource of Gateway cloning, many Gateway compatible binary vectors (Destination vectors) have been advanced in several laboratories and in the current review that are summarized [22]. With the aim of providing tools for high throughput gene analysis, the destination vector conveys some functionally useful elements, such as a selection marker, promoter, new replicon or fusion tag, to the final recombination product. In summary, Gateway vectors facilitates fast and reliable DNA cloning to generate promoter-reporter constructs[23] that enable efficient construction of transgenes for high throughput DNA analysis and elucidation of gene function.

We can summarize the different steps involved in Gateway cloning:

1. Gateway BP reaction: PCR-product with flanking *attB* sites (this step can also use other methods of DNA isolation, such as restriction-digestion) + Donor vector containing *attP* sites + BP clonase => Gateway Entry clone, containing *attL* sites, flanking gene of interest

2. Gateway LR reaction: Entry clone containing *attL* sites + Destination vector containing *attR* sites, and promoters and tags + LR clonase => Expression clone containing *attB* sites, flanking gene of interest, ready for gene expression.

Organelle targeting signal

The presence of complex membrane structures in the cell are called organelles, are the functional and structural symbols of eukaryotic cells. Organelles comprehend with precise sets of enzymes and maintain specialized functions. Proteins are transported to their appropriate destinations in the cell organelle (endoplasmic reticulum (ER), peroxisomes, chloroplasts and mitochondria) or outside. Proteins can be targeted to the inner space of an organelle, plasma membrane, different intracellular membranes, or to exterior of the cell via secretion[24][25][26]. The protein itself carry the information i.e. like proteins, lipids, and metabolites as well as information between organelles contained polypeptide chain or folded protein in this delivery process termed as targeting signals. The amino acid residues in the chain that are constantly bounced and permits targeting are called signal peptides or targeting peptides. Synthesis of the proteins initiated in the cytosol. Some are completely synthesized in the cytosol and imported into the mitochondrion, peroxisome, chloroplast, and nucleus via post-translational transport [27]. Other proteins are co-translationally imported into the endoplasmic reticulum.

Signal peptide is a short N-terminus peptide (usually 16-30 amino acids long) [28] the majority are afresh synthesized proteins that are designed towards the secretory pathway [29]. Signal peptides of target proteins are specifically recognized by SRP (signal recognition particle) as they emerge from the ribosome[30]:[31] Typical signal peptides have a tripartite structure with a 9- to 12-residue-long hydrophobic stretch in the middle[32]:[33] that adopts an α -helical transmembrane (TM) conformation. Moreover,

the hydrophobic part of the signal peptide is crucial for binding to SRP and directs the secretory proteins into the SecB pathway. After translation of signal sequence-ribosome-mRNA complex to the SRP receptor, which is present on the surface of either the plasma membrane (in prokaryotes) or the ER (in eukaryotes) (Gilmore R. et al., 1982) transfers the ribosome nascent chain (RNC) complex from SRP to the translocon (Sec61 complex) and the signal peptides are cleaved off by signal peptidases during or after translocation through the inner membrane (IM) of ER lumen [30].

If Proteins are made in the cytosol (don't enter ER during translation), may be transported to other non-endomembrane destinations (mitochondria, chloroplasts, peroxisomes, and nucleus) permanently and distributed after finishing translation.

ER retention signal

Various molecular signals or protein motif are typically required to retain proteins within the ER[34]. In particular, the HDEL (his-asp-glu-leu) and KDEL (lys-asp-glu-leu) ER retention signals are most widely used signal for retention of proteins in yeast and animal (Elizabeth Hood. et al., 2012). Proteins having C-terminal KDEL-or HDEL interact with the KDEL receptor (act as retrotransport chaperone), a transmembrane protein that functions in vesicular trafficking primarily between the ER and the Golgi shown in the functions and regulation of model KDEL receptor (Fig 1.3).

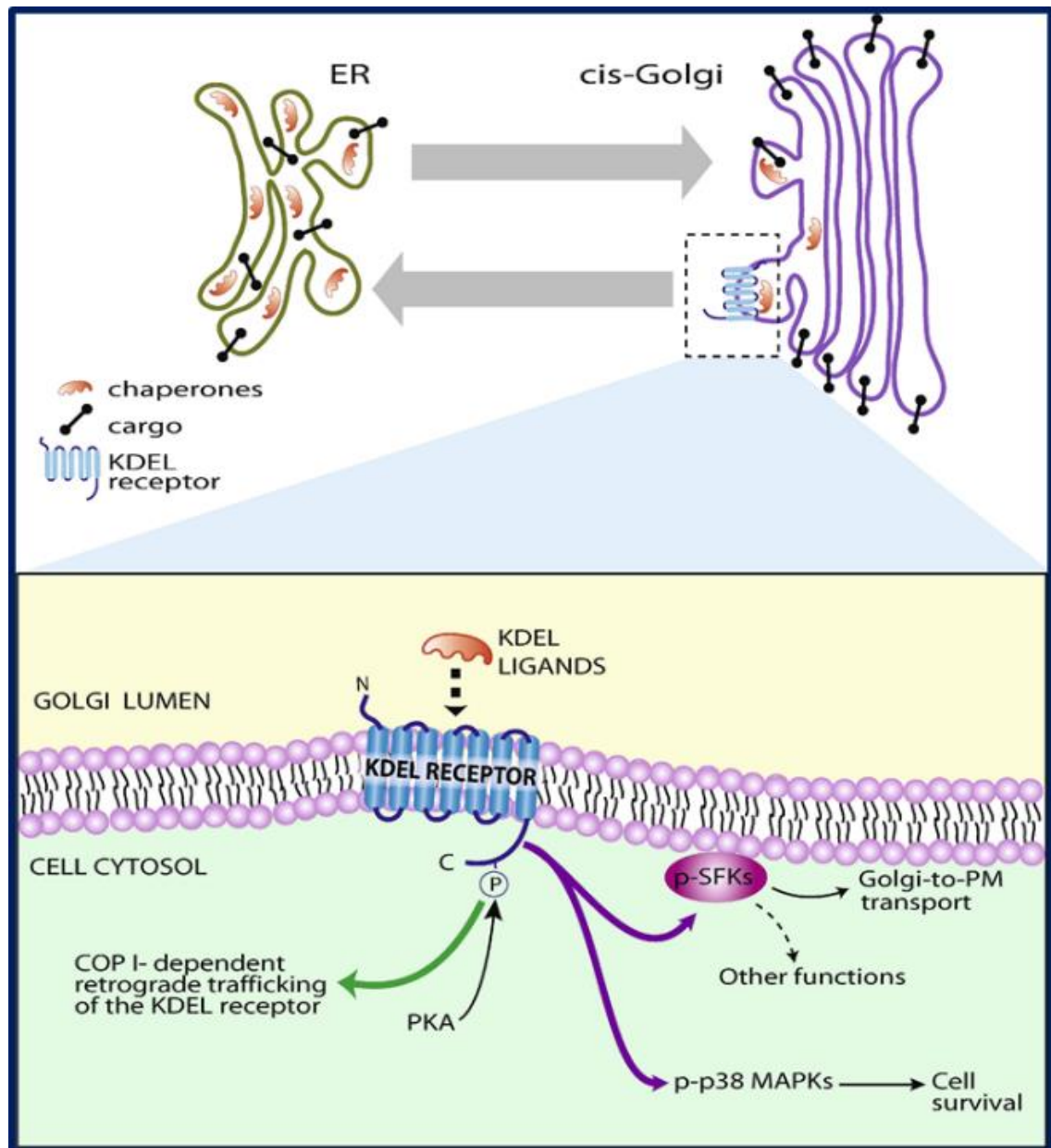


Fig. 1.3. Model of the KDEL receptor functions and their regulation. Chaperones (the KDEL ligands) containing KDEL sequences (red, umbrella-shaped) can leave the ER during normal anterograde transport or cell stress. On arrival at the cis-Golgi, they bind to the KDEL receptor, triggering phosphorylation of SFKs (p-SFKs) spell out SFK at first appearance and p38 MAPKs (p-p38 MAPKs) spell out MAPK at first appearance. SFK activation is required for Golgi-to-plasma-membrane transport, and it appears relevant for the regulation of other cellular functions, while activation of MAPK signaling can promote cell survival. Crosstalk of the KDEL receptor with PKA spell out PKA at first appearance arises via PKA-dependent phosphorylation of the C-terminal of the KDEL receptor, which also appears to be relevant for the modulation of COPI-dependent retrograde transport of

the KDEL receptor [Cited from [M. Capitani and M. Sallèse (2009) *New functions for an old protein, FEBS Lett.*, vol. 583, no. 23, pp. 3863–3871] [35].

erd1 (ER retention defective) mutant 1 and *erd2* (ER retention defective) mutant 2[36][37] are two ER-retention defective mutants for identification of the HDEL receptor and the components involved in the ER-retention system. In Arabidopsis from an early Golgi complex location, retrieval facilitated by both signals certainly arises and demonstrated by reporter proteins comprising Golgi-specific modifications of the N- or O-linked carbohydrate side chains[38][39][40]. KKXX are short carboxy-terminal signals located in cytoplasm, play a crucial role for the localization in the endoplasmic reticulum (ER) of eukaryotic cells. It has many soluble proteins located in the cisternal lumen and of type I transmembrane proteins, respectively[41][42][40].

ER-directing signal peptide (SP_{FMV}) has quite low translocation efficiency compared with SPs (SP_{spo}, SP_{cal}, SP_{clv}) of well-characterized plant proteins of sporamin, calreticulin and CLAVATA3. When GFPs flanked with the N-terminal SPs and a C-terminal ER retention signal (GFP:HDEL without an N-terminal SP used as control, the construct of SP_{spo}GFP:HDEL, SP_{cal}GFP:HDEL and SP_{clv}GFP:HDEL predominantly localized in the ER, whereas SP_{FMV}GFP:HDEL distributed throughout the cytosol, but not to the ER indicate the functional difference in ER translocation between SP_{FMV} and the other SPs shown (Fig 1.4)[43]. Moreover, the ER translocation ability of these SPs using N-glycosylation, increase in the molecular weight of the translocated protein.

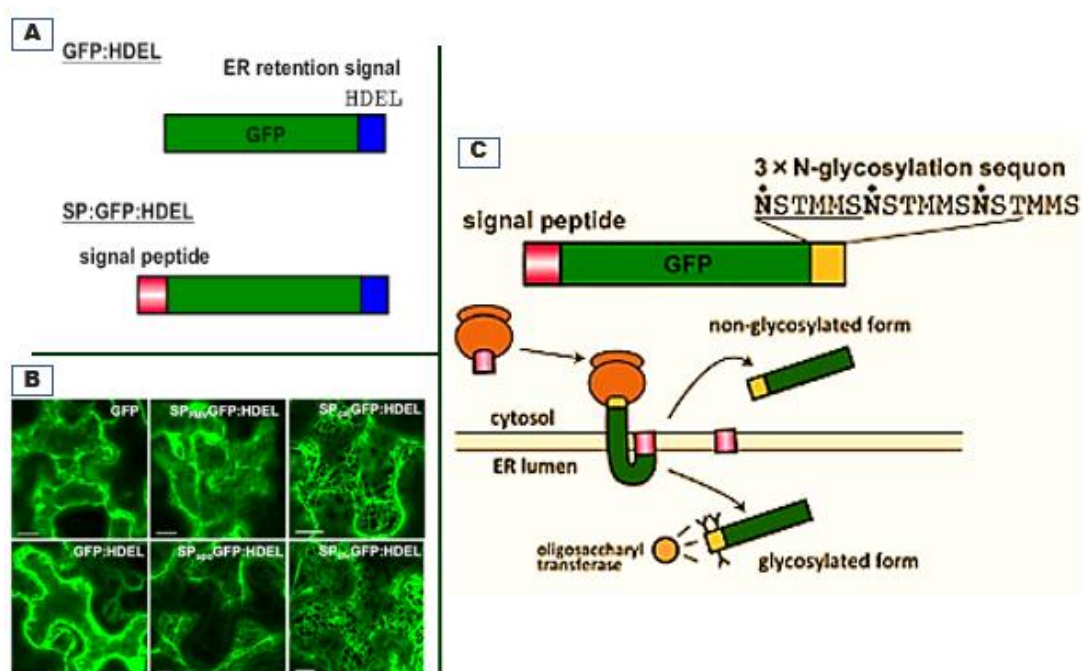


Fig. 1.4. ER translocation efficiency of SP_{FMV} differs from those of plant protein SPs. (A) Schematic representation of fusion proteins for investigating ER translocation efficiency. (B) Cells expressing free GFP, GFP: HDEL, SP_{FMV}GFP:HDEL, SP_{spo}GFP:HDEL, SP_{cal}GFP:HDEL and SP_{clv}GFP:HDEL (C) Schematic representation of the experimental system and fusion proteins with a 3×N-glycosylation sequon. Dots indicate asparagine residues expected to be glycosylated. SPs of MP_{FMV}, sporamin A, calreticulin or CLAVATA3 were fused to the N terminus of GFP:glc, GFP carrying a 3×N-glycosylation sequon in its C terminus (SP_{FMV}GFPglc, SP_{spo}GFPglc, SP_{cal}GFPglc and SP_{clv}GFPglc, respectively). [Cited from: Ishikawa K, et al (2017), *PLOS Pathogens*, 13(6)[43].

Nucleus Localization Signal (NLS)

A nuclear localization signal or sequence (NLS) is one or more short amino acid sequences of positively charged lysines or arginines that import a protein into the cell nucleus by nuclear transport. NLS is the best characterized transport signal for nuclear protein import, which consists of either one (monopartite) or two (bipartite) stretches of basic amino acids[44][45]. Monopartite NLSs are represented by the SV40 large T antigen NLS (The first NLS to be discovered and sequence is ¹²⁶PKKKRRV¹³² at N-terminal region[44] and consists of a highly basic stretch of amino acids Pro-Lys-Lys-Lys-ArgLys-Val and bipartite cNLSs are exemplified by the nucleoplasmin NLS (two clusters of basic amino acids, separated by a spacer of about 10 amino acids sequence is ¹⁵⁵KRPAATKKAGQAKKKK¹⁷⁰)[46]. Both signals are recognized by importin α [47]. Importin α contains a bipartite NLS itself, which is specifically recognized by importin β in fig 1.5[48][49]. The latter can be considered the actual import mediator (Fig 1.5). Nuclear import depends on an importin protein[50] that drifts around in the cytosol and nuclear localization signal on a ‘cargo’ protein[47][51] binds with it.

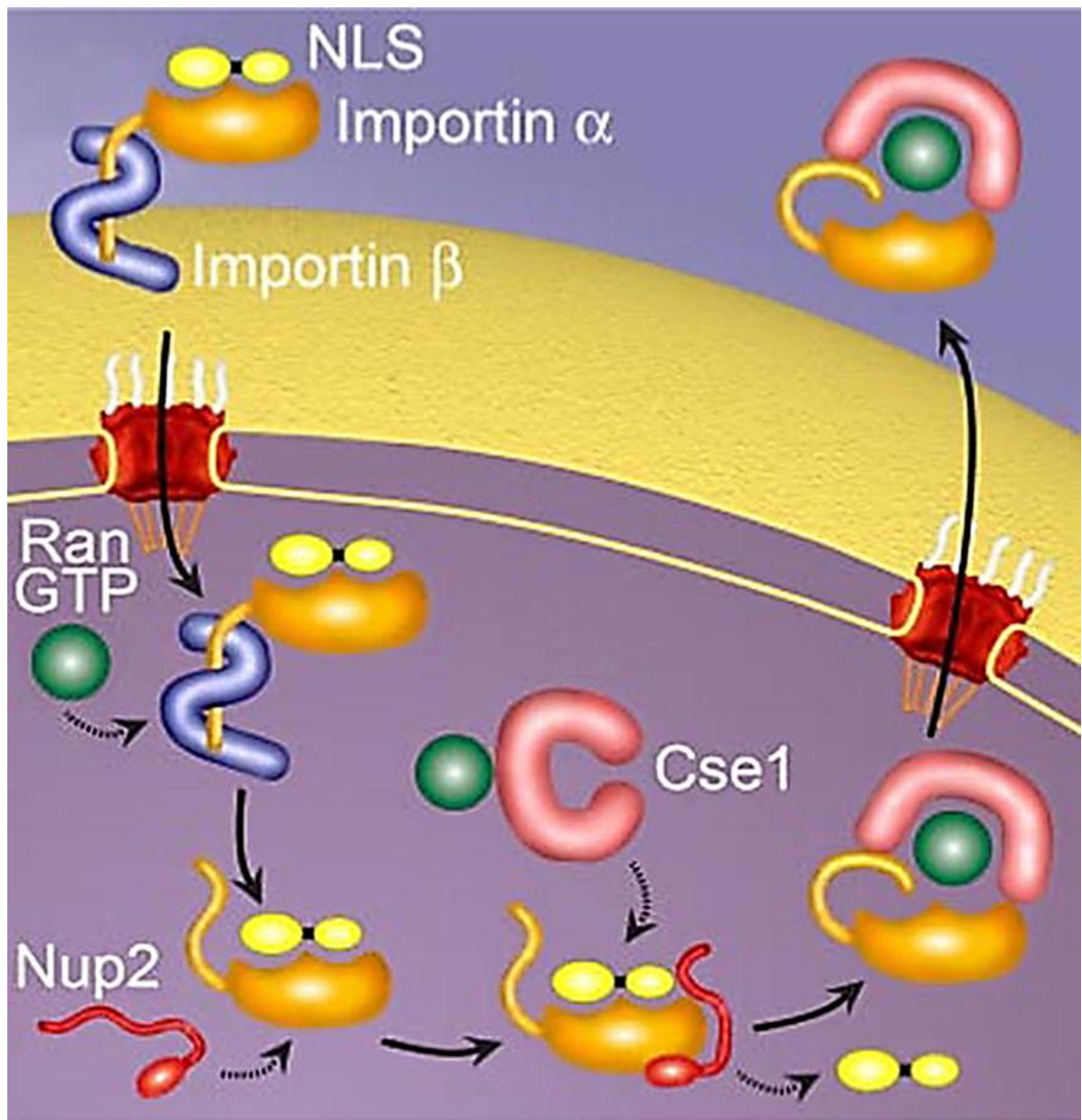


Fig 1.5. The classical nuclear import cycle. In the cytoplasm, cargo containing a cNLS is bound by the heterodimeric import receptor, importin α . Importin α recognizes the cNLS, and importin β mediates interactions with the nuclear pore during translocation. Once inside the nucleus, RanGTP binding causes a conformational change in importin β , which releases the IBB region of importin α . This autoinhibitory domain, together with Nup2 and Cse1, facilitates cNLS dissociation and delivery of the cNLS cargo in the nucleus. Finally, importin α is recycled back to the cytoplasm by the export receptor, Cse1, in complex with RanGTP. [Cited from: [Cited from: A. Lange *et al*, (2007), *J. Biol. Chem.*, vol. 282, no. 8, pp. 5101–5105][49].

Classical nuclear import pathway is the best characterized metabolic systems where importin binding the NLS is energetically downhill as a set mouse trap, ready to spring shut. Actually, classical basic nuclear localization signal (NLS) containing protein is imported by a heterodimeric import receptor having the β -karyopherin importin β that facilitates connections with the nuclear pore complex, and the adaptor protein importin α , that directly binds the classical NLS. In recent years, some nuclear localization signals have been found to be more complex regarding their structures and compositions than that of the SV40 T-antigen signal. Moreover, Sequences distant from a nuclear localization signal can affect its ability to function. After all, NLS hardly enhances gene expression efficiency, because of its disability to promote DNA packaging-unpacking, cell binding, internalization, and endosomal escape[52].

Peroxisome Targeting Signals (PTS)

Peroxisomes are almost universal organelles bounded by a single membrane. Their role diverges from organism to organism but continually comprises the β -oxidation of fatty acids[53]. Peroxisomal protein matrixes are synthesized in the cytoplasm and are targeted to peroxisomes with advantage of a peroxisomal targeting signal (PTS) [54][55]. Peroxisomal proteins are encoded by nuclear genes. Peroxisome targeting signals (PTS) as well as the targeting pathways are preserved to a great range throughout the eukaryotic kingdom.

To date there are two types of known PTS. Type 1 is a carboxyl-terminal (C-terminal) tri- or tetra-peptide (PTS1) with a consensus sequence (S/A/C)-(K/R/H)-(L/A). The most common PTS1 is serine-lysine-leucine (SKL) [53]. Maximum peroxisomal matrix proteins comprise a PTS1 type signal whereas minor group of matrix proteins encompass a conserved nonapeptide that acts as a type 2 (PTS2), is an amino-terminal peptide of nine amino acids, embedded in a longer N- terminal presequence (e.g. RLx5HL) [56][57]. Proteins with a PTS1 are conversant in the cytosol by the soluble receptor Pex5[58][59] and fig 1.6 shows that translocation continued across the peroxisomal membrane until completion Pex5 complex formation shown [60][55].The N-terminal presequence of PTS2-targeted proteins are proteolytically imported into the peroxisomal matrix of plants and mammals, but not into the fungi or trypanosomes[61]. These proteins are recognized by the cytoplasmic receptor Pex7 (Fig 1.6) [62][63][60] and both targeting

pathways merge with a consensus sequence (R/K)-(L/V/I)-XXXXX-(H/Q)-(L/A/F) (where X can be any amino acid).

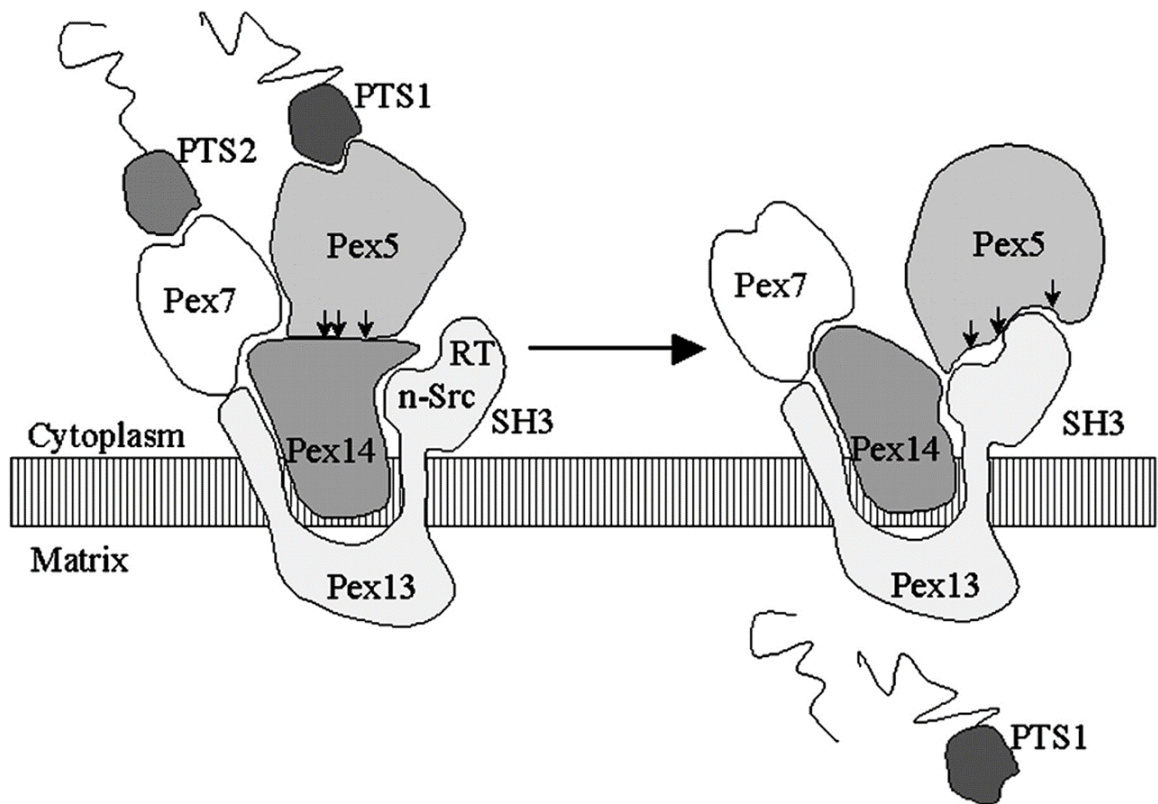


Fig. 1.6. Model for the import of PTS1-containing proteins into the peroxisome. The docking of the PTS1 protein-Pex5p complex at the peroxisome membrane occurs at Pex14p and is mediated by the amino terminus of Pex5p. A region containing the pentapeptide repeats is indicated by arrows. The PTS1 protein is subsequently dissociated and imported into the peroxisome. Concomitant with, or following, this event, Pex5p shifts to the SH3 domain region of Pex13p from which it may recycle to the cytoplasm. Although the fate of Pex7p in this model is not clear, it could be speculated that a similar mechanism might operate commencing with the docking of this protein at Pex14p followed by its displacement to the amino-terminal region of Pex13p. [Cited from: Aaron J. Urquhart *et al.*, (2000). *J. Biol. Chem.*, vol. 275, no. 6, pp. 4127–4136.] [60].

Presequence for Mitochondria targeting

Mitochondria exploit an exclusive mechanism responsible for their explicit targeting and critical sequence motifs involved in protein import from the cytoplasm into the mitochondria were identified from the presequence (PS) of F1-ATPase γ -subunit (pFA γ) in protoplasts. pFA γ contains multiple motifs including N-terminal 77 amino acids of *Arabidopsis thaliana* pFA γ with an alleged processing site that is crucial for protein import into mitochondria. Maximum mitochondrial proteins must be organized to the correct target membrane and typically synthesized as preproteins with signal sequences that are foreseeable by organelle-specific receptors [64][65]. An amino-terminal extension of the preprotein termed the presequence is the most common type mitochondrial targeting signal. In the protein, position of N terminus protein has been recognized as best out of three characterized positions of mitochondrial targeting sequences: the N terminus, internal sequences, and the C terminus. The N-terminal PSs range in size from 15– to 70–amino acid residues and have been demonstrated to be necessary and enough for protein import into mitochondria [66][67]. The PSs have characteristic physicochemical properties with positively charged, hydroxylated and hydrophobic residues, and carry the potentiality to build an amphiphilic α helix [68]. The PSs are ideally suited for interacting with the mitochondrial outer membranes Tom20 [69] shown in Fig 1.7, making a complex with an N-terminal PS discovered that the hydrophobic surface of the amphipathic α -helix binds to the hydrophobic groove [70]. Whereas, in the inner membrane, two TIMs (translocase of the inner membrane of mitochondria) exist for the translocation of precursors in fig 1.7 [71][72].

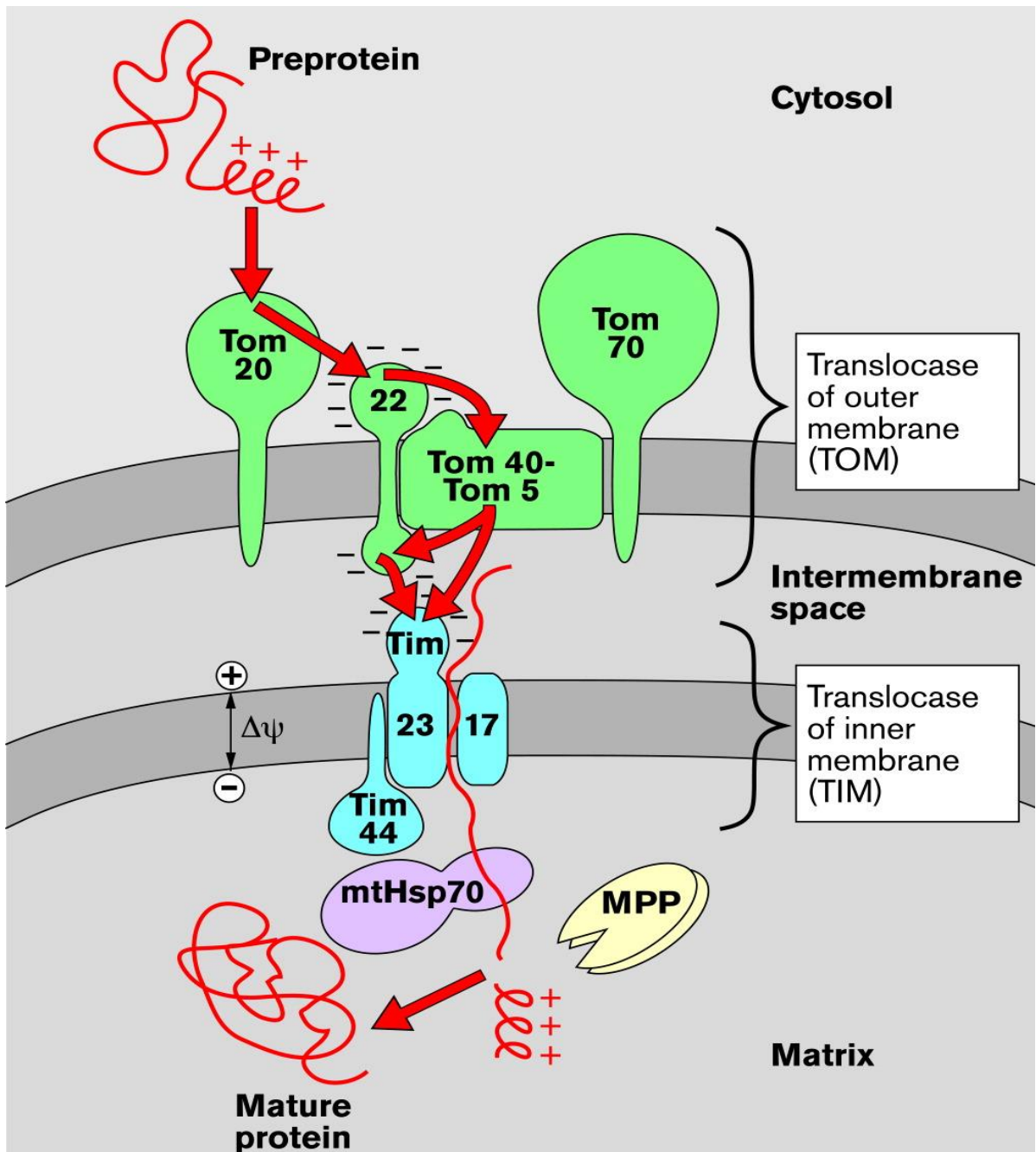


Fig. 1.7. Transport pathway of a presequence-carrying preprotein from the cytosol into mitochondria. The amino-terminal presequence (positively charged) of the preprotein successively interacts with the receptors Tom20 and Tom22, the channel-forming protein Tom40 and the intermembrane space domains of Tom22 and Tim23. The membrane potential $\Delta\psi$ across the inner membrane and the heat shock protein mtHsp70 drive the preprotein into the matrix where the presequence is cleaved off by the mitochondrial processing peptidase (MPP) [Cited from: [N. Pfanner., (2000) *Curr. Biol.*, vol. 10, no. 11, pp. R412–R415] [71].

Malectin Like Domain (MLD)

Malectin is a highly conserved animal lectin from the endoplasmic reticulum (ER) protein with a quality control function in the N-glycosylation pathway (a process in which the nascent glycoproteins have the assisted folding). It has a β -sandwich fold with long loops connecting the β -sheets (Fig 1.8) capable of binding to nigerose, maltose and diglycosylated oligosaccharide, with nigerose as favored ligand [73]. Several carbohydrate-binding modules (CBMs) discovered in other domains that shared sequence homology with the malectin, were classified and grouped as a novel CBM57 family by Carbohydrate-Active Enzymes (CAZy) database[74].

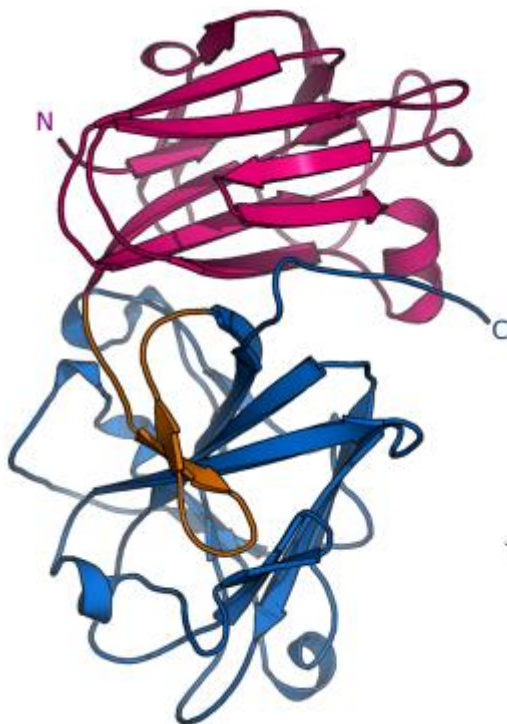


Fig. 1.8. Architecture of the tandem malectin-like ectodomain of ANXUR1. Front and 180° rotated views of the ANX1 ectodomain (ribbon diagram) with mal-N shown in magenta, the β -hairpin in orange and mal-C in blue. [Cited from: Moussu S, *et al.*, (2018), doi: <http://dx.doi.org/10.1101/251959>][74].

In the N-glycosylation pathway the transportation of the unfolded promising glycoproteins happens into the ER lumen where an oligosaccharide with 3 terminal

glucoses is transferred to the protein with Asn-X-Thr/Ser sequence consensus[75]. Malectin participates in N-glycosylation process before the hydrolyse of the second glucose for the purpose of quality control[76] and protect glycoproteins to prevent their degradation[77]. In another study, Malectin preventing the excretion of misfolded proteins to the Golgi and circumventing the establishment of aberrant proteins[78].

Plant malectin-like receptor kinases, known as *Catharanthus roseus* receptor-like kinase 1-like proteins (CrRLK1Ls) (Schulze-Muth et al., 1996), anticipated as potential cell wall sensors and involved in many different plant functions (Franck et al. 2018). All members of the CrRLK1L subfamily contain extracellular domains (ECDs) with similarly two tandem carbohydrate-binding malectin-like domain (MLD), a transmembrane domain (TMD), and an intracellular Ser and Thr kinase domain and role in diverse signaling pathways in algae and plants (Fig 1.9) [79][80][81].

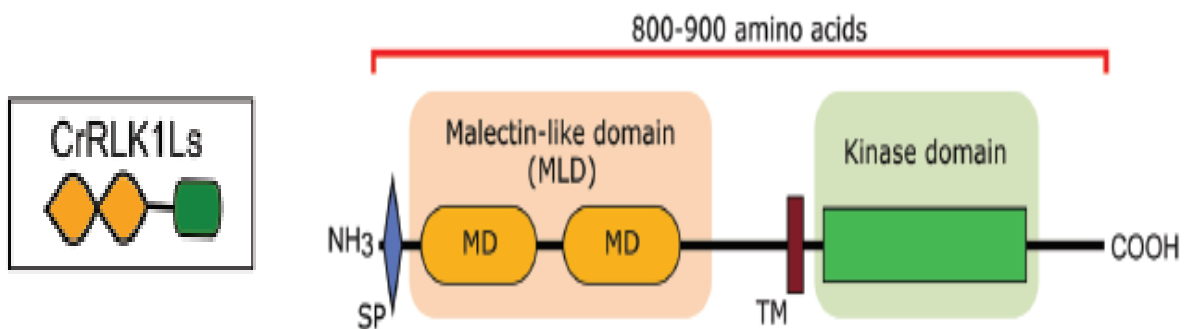


Fig.1.9. Domain organization of the CrRLK1L proteins. Domains are to scale and based on FER as given in the NCBI Conserved Domain Database. SP, signal peptide; MD, malectin domain; TM, transmembrane domain. [Cited from (Galindo-Trigo S, *et al.*, (2016) *Plant Sci.* 7:1269.)][80].

In the RLK family, the MLD encompasses the pivotal ECD in the CrRLK1L, LRK10L-2, LRR-1c, and LRR-1a subfamilies. In the model plant *A. thaliana*, the CrRLK1L subfamily contains 17 members, 10 of which have been characterized: THESEUS1 (THE1), HERCULES1 (HERK1), HERCULES2 (HERK2), FERONIA/SIRENE (FER/SIR), ANXUR1 (ANX1), ANXUR2 (ANX2), ERULUS/[Ca²⁺]_{cyt}-ASSOCIATED PROTEIN KINASE 1 (ERU/CAP1), CURVY1

(CVY1), BUDDHA'S PAPER SEAL1 (BUPS1), and BUDDHA'S PAPER SEAL2 (BUPS2). Moreover, MLDs are exceedingly deviating in primary sequence, suggesting efficient divergence, maintenance of predicted secondary assemblies. From a couple of years, great progress has been made in the field, especially in the context of FER, THE1, ANX1, and ANX2. RALF peptides, glycosylphosphatidylinositol (GPI)-anchored proteins, RAC/ROP GTPases, and receptor-like cytoplasmic kinases (RLCKs), as well as ROS and Ca²⁺ signaling are the common signaling elements of plant malectin-like receptor kinases. The novel interactors for FER have been discovered, including some FER ligands (Fig 1.10) that focuses on common downstream signaling partners, and subsequently discusses evolutionary aspects of CrRLK1Ls [82].

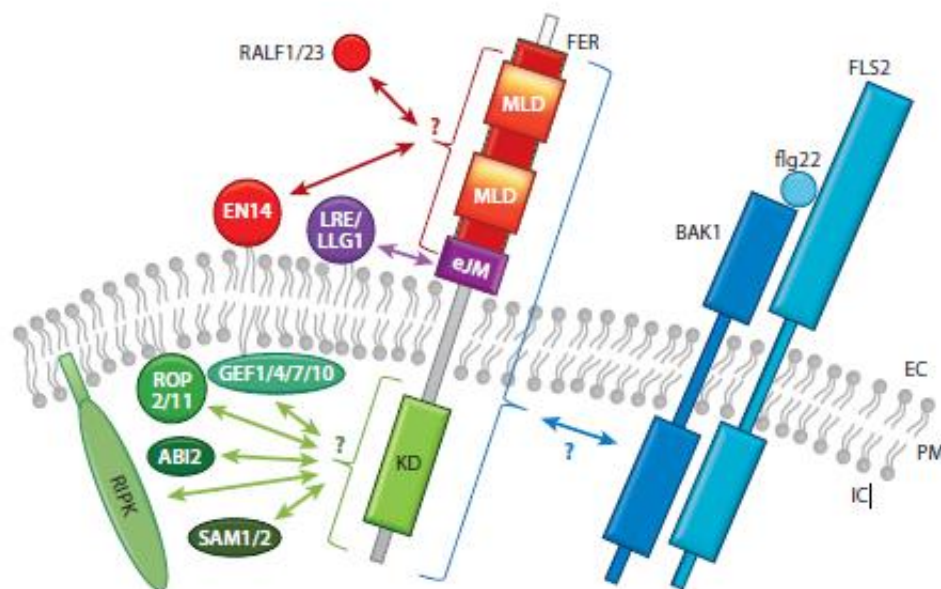


Fig 1.10. Summary of FER-associated proteins. A schematic representation of FER-associated proteins is shown, including the corresponding FER-binding domains. Abbreviations: ABI2, ABSCISIC ACID INSENSITIVE 2; BAK1, BRASSINOSTEROID INSENSITIVE 1 ASSOCIATED KINASE 1; EC, extracellular; EN14, EARLY NODULIN 14; eJM, extracellular juxta-membrane domain; FER, FERONIA; flg22, flagellin epitope 22; FLS2, FLAGELLIN SENSING 2; GEF1/4/7/10, GUANINE NUCLEOTIDE EXCHANGE FACTOR 1/4/7/10; IC, intracellular; KD, kinase domain; LRE/LLG1, LORELEI and LORELEI-LIKE GPI-ANCHORED PROTEIN 1; MLD, malectin-like domain; PM, plasma membrane; RALF1/23, RAPID ALKALINIZATION

FACTOR 1 and 23; RIPK, RESISTANCE TO PSEUDOMONAS SYRINGAE PV. MACULICOLA 1-INDUCED PROTEIN KINASE; ROP2/11, RHO-GTPASE OF PLANTS 2 and 11; SAM1/2, S-ADENOSYLMETHIONINE SYNTHASE 1 and 2. [Cited from: Franck et al. (2018), *Annu. Rev. Plant Biol.* 69:301–28][82].

Chapter 2

Gateway Binary Vectors with Organelle-Targeted Fluorescent Proteins for Highly Sensitive Reporter Assay in Gene Expression Analysis of Plants

1. Introduction

Fluorescent proteins are the versatile probes in live imaging and become an essential tool for cell biology and physiology. In addition to the normal types, fluorescent proteins fused with organelle-targeting signals were widely used for analysis of subcellular localization of proteins and organelle dynamics in living organisms including plants. Experiments using GFP fused with PTS1 or PTS2 revealed that directional movement of peroxisomes depends on actin filaments in *A. thaliana* [83][84]. Analysis using GFP fused with mitochondrial presequences from *A. thaliana* CPN60, *Nicotiana plumbaginifolia* β -ATPase, and yeast COX 4p showed different mobility and shape of mitochondria in plant cells depending on the location, developmental stage, and physiological conditions[85][86]. GFP fused with a signal sequence and an ER retention signal was used to analyze the ER body, a characteristic structure derived from ER under stress conditions, in *A. thaliana*[87]. Because the accumulation of fluorescent proteins in organelles brings brighter and distinctive signals, organelle-targeted fluorescent proteins were also used in promoter:reporter experiments for visualization of target tissues or cells by a specific promoter, and for precise expression analysis of unidentified promoters. Usually, nucleus-targeted fluorescent proteins are used for these purposes and many plant promoters were analyzed by nucleus-targeted GFP (Goh et al., 2012; Ortiz-Morea et al., 2016). Recently, Gateway cloning has become one of the most widely used techniques to clone DNA fragments into vectors for many research fields including plants[88][88][89][90][91][92][93]. In the Gateway cloning technology, two types of promoter entry clones are mostly used for different cloning strategies. The *attL1*-promoter-*attL2* entry clone is used to prepare simple constructs such as promoter:reporter (*attB1*-promoter-*attB2*-reporter), whereas, the *attL4*-promoter-*attR* 1 entry clone is usually used for combinatorial cloning with *attL1*-cDNA-*attL2* to prepare promoter:cDNA-reporter (*attB4*-

promoter-*attB1*-cDNA-*attB2*- reporter) constructs. Previously, we have developed series of Gateway binary vectors (pGWBs) compatible with Gateway cloning technology for construction of fusions with many kinds of tags, epitopes, GUS, LUC, and fluorescent proteins including sGFP, EYFP, ECFP, G3GFP, mRFP and TagRFP[94]. In addition to the pGWB series carrying *attR1-attR2* sites for LR reaction with an *attL1*-promoter-*attL2* entry clone[95][96][97][98], we also developed R4L1pGWB series carrying *attR4-attL1* acceptor sites specialized for creation of promoter:reporter constructs by an LR reaction with *attL4*-promoter-*attR1* entry clone[99][100]. These vectors have been frequently used in promoter assays of transgenic plants by microscopic observation of visible reporters, GUS, and fluorescent proteins to determine the organs, tissues, and cells expressing a gene of interest in detail. In this study, we developed new pGWBs (*attR1-attR2* acceptor sites) and R4L1pGWBs (*attR4-attL1* acceptor sites) carrying organelle-targeted sGFPs (ER-, nucleus-, peroxisome-, and mitochondria-targeted sGFPs) and organelle-targeted TagRFPs (nucleus-, peroxisome-, and mitochondria-targeted TagRFPs) to facilitate promoter:reporter assays in plants. We also tested the performance of these vectors and reported the highly sensitive detection of fluorescence signals with nucleus- and peroxisome-targeted sGFP compared with normal sGFP (no organelle-targeted type) in promoter:reporter analysis using transgenic plants.

2. Materials and Methods

Plasmid constructions

Plasmids were constructed according to standard methods[101]. KOD DNA polymerase (Toyobo, Osaka, Japan) was used for PCR to prepare amplified products with blunt ends. The sequences of the PCR-amplified regions and ligation junctions were confirmed by sequence analysis. All primers used in this study are listed in Table 2.1. Synthetic green fluorescent

protein (sGFP)[102] was amplified using pGWB404[95] as a template with the primers sGFP-F and sGFP-R. Amplified DNA was introduced into R4L1pUGW1[99] to make R4L1pUGW4 (R4-L1-sGFP). ER-targeted sGFP (ER-sGFP) sequence was amplified using pNMG3 (the signal peptide of *A. thaliana* endo-xyloglucan transferase plus sGFP hooked with the HDEL retention signal at the C terminus)[103][103] as a template with the primers ER-sGFP-F and ER-sGFP-R.

Nucleus-targeted sGFP (NLS-sGFP, carrying nuclear localization sequence PKKKRKV at N-terminal region) was amplified using 35SΩ-NLS-sGFP(S65T) [102](Chiu et al., 1996) as a template with the primers NLS-sGFP-F and sGFP-R. Peroxisome-targeted sGFP (Px-sGFP, carrying peroxisome-targeting sequence SKL at C-terminal) was amplified using pGWB404 as a template with the primers sGFP-F and Px sGFP-R. Nucleus-targeted TagRFP (NLS-TagRFP, carrying PKKKRKV at N-terminal region) was amplified using pGWB659 [97] as a template with the primers NLS-TagRFP-F and TagRFP-R. Peroxisome-targeted TagRFP (Px-TagRFP, carrying SKL at C-terminal) was amplified using a pGWB659 as a template with the primers TagRFP F and Px-TagRFP-R. Mitochondria-targeted sGFP and TagRFP (Mt-sGFP and Mt-TagRFP), carrying N-terminal 57 amino acids of *A. thaliana* F1 ATPase γ subunit [104] were synthesized by GeneArt Gene Synthesis (Thermo Fisher Scientific, Kanagawa, Japan). These DNA fragments were introduced into *Aor51HI* site of pUGW2[95] and R4L1pUGW1 (Nakamura et al., 2009) to make pUGW62 (R1-R2-ER-sGFP), pUGW65 (R1-R2-NLS-sGFP), pUGW68 (R1-R2-Px-sGFP), pUGW71 (R1-R2-Mt-sGFP), pUGW85 (R1-R2-NLS-TagRFP), pUGW88 (R1-R2-Px-TagRFP), pUGW91 (R1-R2-Mt-TagRFP), R4L1pUGW62 (R4-L1-ER-sGFP), R4L1pUGW65 (R4-L1-NLS-sGFP), R4L1pUGW68 (R4-L1-Px-sGFP), R4L1pUGW71 (R4-L1-Mt-sGFP), R4L1pUGW85 (R4-L1-NLS-TagRFP), R4L1pUGW88 (R4-L1-Px-TagRFP), and R4L1pUGW91 (R4-L1-

MtTagRFP), respectively. The DNA fragments containing *attR1-Cm^r-ccdB-attR2*-reporter prepared from resulting pUGWs and DNA fragments containing *attR4-Cm^r-ccdB-attL1*-reporter prepared from resulting R4L1pUGWs were introduced into pGWB400, pGWB500[96], pGWB600[97] and pGWB700[100] for construction of destination vectors pGWBs and R4L1pGWBs indicated in Fig.2.1. The Cm^r is the chloramphenicol resistance and *ccdB* is the control of cell death used as a negative selection marker in *E. coli*. Transformed *E. coli* DB3.1 (Thermo Fisher) were selected on Luria broth (LB) media containing appropriate antibiotics (30 mg/L of chloramphenicol, 50 mg/L of ampicillin, or 100 mg/L of spectinomycin).

2.2. Preparation of entry clones and expression constructs

The DNA fragment of the cauliflower mosaic virus 35S promoter was amplified using pGWB402[95] as a template with the primers 35Spro-attB4F and 35Spro-attB1R. The DNA fragment of 3-ketoacyl-CoA thiolase 2 (KAT2, AT2G33150) promoter spanning -2074 to +6 (A of ATG is +1) was amplified using genomic DNA of *A. thaliana* (Col-0 accession) as a template with the primers KAT2pro-GWB4F and KAT2proGWB1R. These DNA fragments were applied for second PCR with the primers attB4-adapt and attB1R-adapt and introduced into pDONR P4-P1R (Thermo Fisher) by BP reaction to make *attL4-Pro35S-attR1* and *attL4-ProKAT2-attR1* entry clones. The DNA fragment of DAD1-LIKE LIPASE2 (DALL2, AT1G51440) promoter spanning -2413 to +10 was amplified using genomic DNA of *A. thaliana* (Col-0 accession) with DAL2-2413FattB4 and DAL2-21RattB1 primers and introduced into pDONR P4-P1R by BP reaction to make an *attL4-ProDALL2-attR1* entry clone. The *attL1-ProMYB21:MYB21-attL2* entry clone carrying promoter and coding sequence of MYB21 (AT3G27810) was prepared as described in Reeves et

al. (2012)[105]. Transfer of the DNA fragment from entry clones to pGWB or R4L1pGWB was performed by LR reaction according to the manufacturer's instruction.

2.3. Transient expression analysis using Japanese leek

Two expression constructs were mixed at 1:1 w/w ratio and introduced into Japanese leek epidermal cells using particle bombardment technique as described in Hino et al. (2011)[106].

2.4. Generation of transgenic *A. thaliana* for stable expression analyses.

Transformation of *Agrobacterium tumefaciens* C58C1 (pMP90) was carried out using the freeze-thaw method[107]. Transformation of *A. thaliana* (Col 0 accession) was performed by floral inoculating protocol[108] and inoculated plants were grown at 22 °C under long day photoperiod (16 hr light /8 hr dark cycle). Harvested T0 seeds were vernalized at 4 °C for 2-3 days and grown on Murashige and Skoog (MS) agar medium containing kanamycin (30 mg/L) or hygromycin (20 mg/L) or BASTA (0.0054 %) with Cefotax (100 mg/L) (Chugai Pharmaceutical Co., Tokyo, Japan) at 22 °C under continuous light conditions. Two-week-old kanamycin- or hygromycin-resistant seedlings (T1) were transplanted to Jiffy-7 (Jiffy Preforma Production K. K, Yokohama, Japan) and grown at 22 °C under long-day photoperiod. Ten-day-old BASTA-resistant seedlings (T1) were transferred to BASTA- and Cefotax-free plates to enhance root elongation. After 7 days, the seedlings were transplanted to Jiffy-7 and grown at 22 °C

under long-day photoperiod. Homozygous T3 plants harboring transgene were used for expression analyses.

2.5. Expression analyses by confocal microscopy and measurement of fluorescence intensity

Fluorescence signals were examined with a TCS SP5 confocal laser-scanning microscope (Leica Microsystems, Wetzlar, Germany) using an HCX IRAPO L 25.0×0.95 water-immersion objective lens. sGFP was excited with the argon laser line (488 nm) and TagRFP was excited with helium-neon laser line (543 nm). The fluorescence from sGFP and TagRFP were detected at 500-530 nm and 555-615 nm, respectively. The images were obtained using the sequential scanning mode with a resolution of 1024×256 pixels with bidirectional scanning mode at speed of 200 Hz for transient expression analysis and 512×512 pixels at the speed of 400 Hz for stable expression analysis. For analysis of wound induced expression, leaves were scratched with tweezers as described in Ruduś et al. (2014)[109] and the adjacent regions were observed after 150 min. For analysis of dark-induced expression, plants were moved to a dark chamber and leaves were observed after 2 hours. Fluorescence intensities were quantified with the Leica Application Suite Advanced Fluorescence (LAS AF) software according to the manufacturer. Mean gray values of GFP fluorescence were calculated in each of three randomly selected ROI (1,000 μm^2).

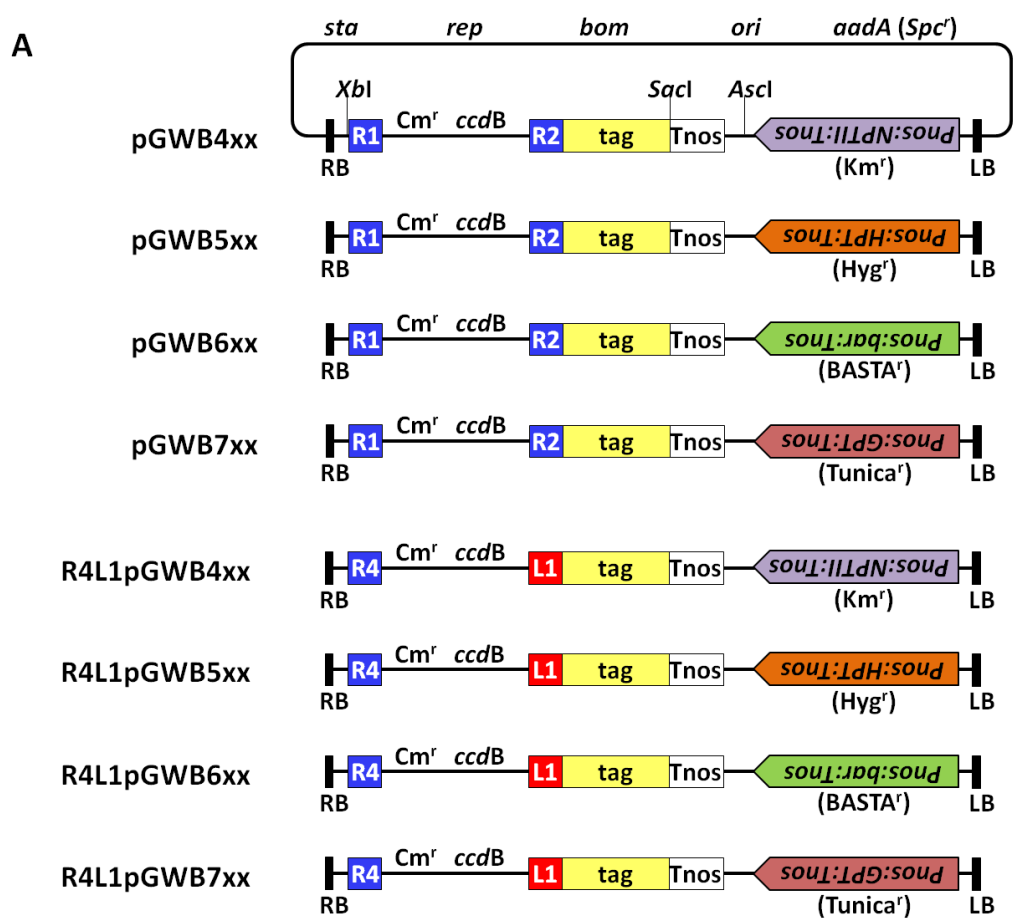
Table 2.1. Oligonucleotides used in this study.

Oligos	Sequence
sGFP-F	5'-ATGGTGAGCAAGGGCGAG-3'
sGFP-R	5'-TTACTTGTACAGCTCGTCCA-3'
ER-sGFP-F	5'-ATGACTGTTTCTTCATCTCCAT-3'
ER-sGFP-R	5'-TTAAAGCTCATCATGCTTGTAC-3'
NLS-sGFP-F	5'-ATGGCTCCAAAGAAGAAGAG-3'
Px-sGFP-R	5'-TCATAGCTTCGACTTGTACAGCTCGTCCAT-3'
NLS-TagRFP-F	5'-ATGGCTCCAAAGAAGAAGAGAAAGGTCATGGTGTCTAAGGGCGAAG-3'
TagRFP-R	5'-TCAATTAAGTTTGTGCCCCAG-3'
TagRFP-F	5'-ATGGTGTCTAAGGGCGAAG-3'
Px-TagRFP-R	5'-TCATAGCTTCGAATTAAGTTTGTGCCCCAG-3'
35Spro-attB4F	5'-ATAGAAAAGTTGGCTGAGACACTGCATGCCTGCAGGTCCCC-3'
35Spro-attB1R	5'-TTTGTACAAACTTGTGACACTAGCGTGCCTCTCCAAATG-3'
KAT2pro- GWB4F	5'-ATAGAAAAGTTGTTTATTACAGTTCCACGTGGTAT-3'
KAT2pro- GWB1R	5'-TTTGTACAAACTTGTCTCCATTTTTTCCGGCTGAT-3'
attB4-adapt	5'-GGGGACAACCTTTGTATAGAAAAGTTG-3'
attB1R-adapt	5'-GGGGACTGCTTTTTTGTACAAACTTG-3'
DAL2- 2413FattB4	5'-GGGACAACCTTTGTATAGAAAAGTTGCCCTGGAGACACAGGTGAGTTGTCTTTG-3'
DAL2-21RattB1	5'-GGGGACTGCTTTTTTGTACAAACTTGGAGAAGCCATTTAGATTGGGTTGTTTGTGAGAG-3'

3. Results and discussion

3.1. Gateway binary vectors with an organelle-targeted fluorescent protein as a reporter

We developed Gateway binary vector series carrying an organelle targeted sGFP or TagRFP for promoter:reporter analysis in plants. The sequences fused to fluorescent proteins for organelle localization were the signal peptide of *A. thaliana* endo-xyloglucan transferase and HDEL retention signal for ER-targeted sGFP (ER-sGFP), PKKKRKV for nucleus-targeted sGFP (NLS-sGFP) and TagRFP (NLS-TagRFP), SKL for peroxisome-targeted sGFP (Px-sGFP) and TagRFP (Px-TagRFP) and first to 57th amino acid residues including presequence of *A. thaliana* F1ATPase γ subunit for mitochondria-targeted sGFP (Mt-sGFP) and TagRFP (Mt-TagRFP). Fig. 2.1 shows the schematic structure of the 56 vectors constructed in this study. The pGWB series contain *attR1-attR2* acceptor sites compatible with an *attL1*-promoter-*attL2* entry clone for preparation of an *attB1*-promoter-*attB2*-reporter construct. The R4L1pGWB series contain *attR4-attL1* acceptor sites compatible with *attL4*-promoter-*attR1* entry clone for preparation of an *attB4*-promoter-*attB1*-reporter construct. Both pGWB and R4L1pGWB were designated as 4xx, 5xx, 6xx and 7xx, where 4, 5, 6, and 7 represent four kinds of plant selection markers consistent with previously developed pGWBs and R4L1pGWBs[96],[97],[100]. In this system, 4xx refers to neomycin phosphotransferase II (NPTII) conferring kanamycin resistance (Km^r), 5xx indicates hygromycin phosphotransferase (HPT) conferring hygromycin resistance (Hyg^r), 6xx refers to bialaphos resistance gene (*bar*) conferring BASTA resistance ($BASTA^r$), and 7xx indicates UDP-N-acetylglucosamine: dolichol phosphate N-acetylglucosamine-1-P transferase (GPT) conferring tunicamycin resistance ($Tunica^r$). These marker genes were placed in reverse orientation under regulation of the nopaline synthase (*nos*) promoter and followed by *nos* terminator (Fig. 2.1A). The last two digits represent the reporter type of organelle-targeted fluorescent proteins; 62 for ER-sGFP, 65 for NLS-sGFP, 68 for Px-sGFP, 71 for Mt-sGFP, 85 for NLS-TagRFP, 88 for Px-TagRFP and 91 for Mt-TagRFP (Fig. 2.1B). The complete nucleotide sequence of pGWBs and R4L1pGWBs developed in this study appears in GenBank/EMBL/DDBJ databases under accession nos. AP018976 to AP019003 for pGWBs and AP018948 to AP018975 for R4L1pGWBs. The pGWBs and R4L1pGWBs developed in this work are available through RIKEN BRC Experimental Plant Division (<https://epd.brc.riken.jp/en/>).



B

ER-sGFP	NLS-sGFP	Px-sGFP	Mt-sGFP
pGWB462	pGWB465	pGWB468	pGWB471
pGWB562	pGWB565	pGWB568	pGWB571
pGWB662	pGWB665	pGWB668	pGWB671
pGWB762	pGWB765	pGWB768	pGWB771
R4L1pGWB462	R4L1pGWB465	R4L1pGWB468	R4L1pGWB471
R4L1pGWB562	R4L1pGWB565	R4L1pGWB568	R4L1pGWB571
R4L1pGWB662	R4L1pGWB665	R4L1pGWB668	R4L1pGWB671
R4L1pGWB762	R4L1pGWB765	R4L1pGWB768	R4L1pGWB771
	NLS-TagRFP	Px-TagRFP	Mt-TagRFP
	pGWB485	pGWB488	pGWB491
	pGWB585	pGWB588	pGWB591
	pGWB685	pGWB688	pGWB691
	pGWB785	pGWB788	pGWB791
	R4L1pGWB485	R4L1pGWB488	R4L1pGWB491
	R4L1pGWB585	R4L1pGWB588	R4L1pGWB591
	R4L1pGWB685	R4L1pGWB688	R4L1pGWB691
	R4L1pGWB785	R4L1pGWB788	R4L1pGWB791

Fig. 2.1. Schematic illustration of the pGWBs and R4L1pGWBs.

(A) The overall structure of pGWBs and R4L1pGWBs. NPTII (Km^r), HPT (Hyg^r), bar (BASTA^r), and GPT (Tunica^r) are used as plant selection markers for pGWB4xx, pGWB5xx, pGWB6xx and pGWB7xx series, respectively. pGWB and R4L1pGWB vectors contain *attR1-attR2* and *attR4-attL1* acceptor sites, respectively. (B) Organelle-targeted fluorescent proteins used as tags in pGWBs and R4L1pGWBs. ER-sGFP, ER-targeted sGFP; NLS-sGFP, nucleus-targeted sGFP; Px-sGFP, peroxisome-targeted sGFP; Mt-sGFP, mitochondria-targeted sGFP; NLS-TagRFP, nucleus-targeted TagRFP; Px-TagRFP, peroxisome-targeted TagRFP; Mt-TagRFP, mitochondria-targeted TagRFP; RB, right border; LB, left border; Cm^r, chloramphenicol resistance (chloramphenicol acetyl transferase) used for selection in bacteria; *ccdB*, negative selection marker used in bacteria; sGFP, synthetic green fluorescent protein with S65T mutation; TagRFP, Tag red fluorescent protein; *sta*, region for stability in *Agrobacterium tumefaciens*; *rep*, broad host-range replication origin; *bom*, cis-acting element for conjugational transfer; *ori*, ColE1 replication origin; *aadA*, spectinomycin resistance (Spc^r) marker used for selection in bacteria.

3.2. Localization analysis of organelle-targeted TagRFP by transient expression

To confirm the intracellular localization of organelle-targeted TagRFPs constructed in this study, we performed co-localization analysis by transient expression using established localization markers NLS-sGFP[102], Px-sGFP[84] and Mt-sGFP[104] as references. Pro35S:NLS-sGFP, Pro35S:NLS-TagRFP, Pro35S:Px-sGFP, Pro35S:Px-TagRFP, Pro35S:Mt-sGFP, Pro35S:Mt-TagRFP constructs were prepared by LR reaction between an *attL4-Pro35S-attR1* promoter entry clone and R4L1pGWB465, 485, 468, 488, 471, 491, respectively. Pairs of sGFP and TagRFP constructs carrying the same organelle-targeting signal were delivered into Japanese leek epidermal cells by particle bombardment. Confocal microscopic analysis revealed the occurrence of nuclear co-localization of NLS-sGFP and NLS-TagRFP (Fig. 2.2A), peroxisomal co-localization of Px-sGFP and Px-TagRFP (Fig. 2.2B), and mitochondrial co-localization of Mt-sGFP and Mt-TagRFP (Fig. 2.2C). These results clearly indicated a correct localization of newly constructed NLS-TagRFP, Px-TagRFP, and Mt-TagRFP reporters in plant cells.

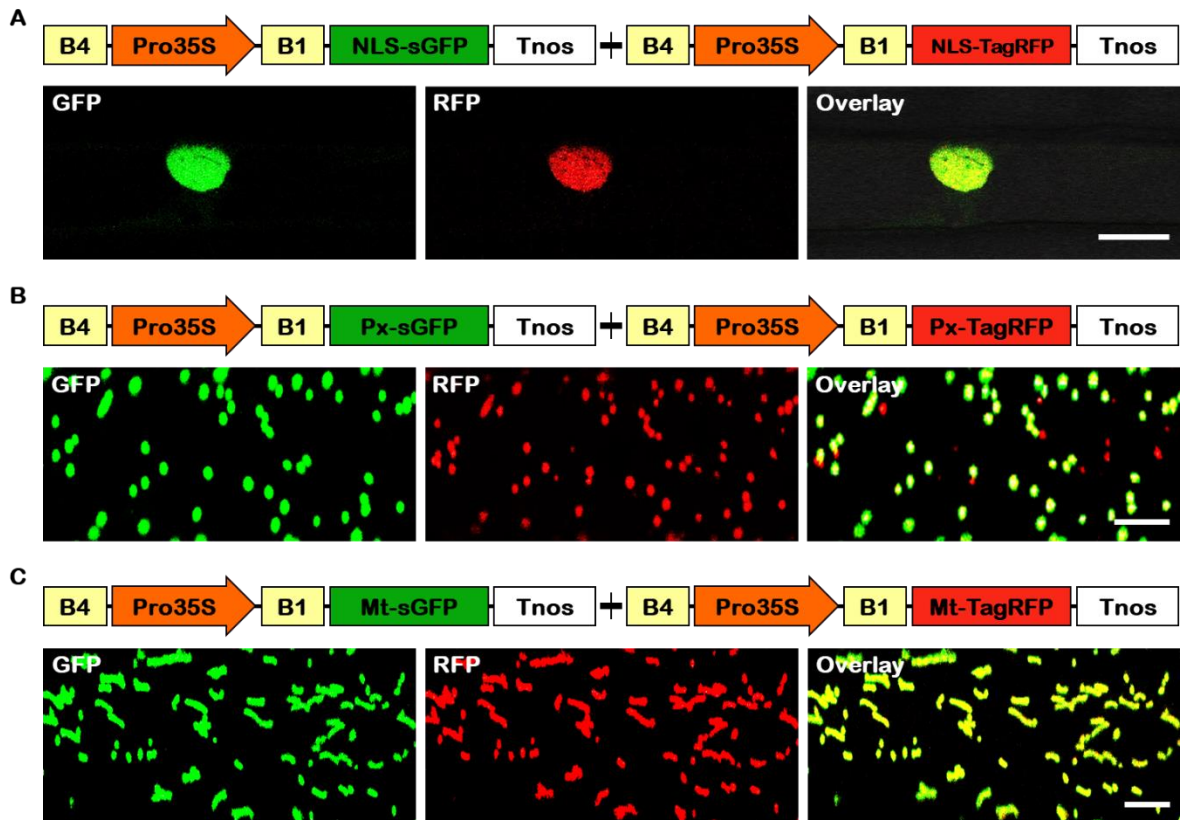


Fig. 2.2. Intracellular localization of organelle-targeted sGFP and TagRFP transiently expressed in Japanese leek epidermal cells. (A) Pro35S:NLS-sGFP + Pro35S:NLS-TagRFP. (B) Pro35S:Px-sGFP + Pro35S:Px-TagRFP. (C) Pro35S:Mt-sGFP + Pro35S:Mt-TagRFP. GFP, signal of sGFP; RFP, signal of TagRFP; Overlay, overlay of GFP and RFP. Scale bars = 10 μ m.

3.3. Expression analysis in transgenic *A. thaliana*

In order to test the performance of newly constructed vectors for highly sensitive detection of gene expression, promoter:organelle-targeted-sGFP or promoter:cDNA-organelle-targeted-sGFP constructs were prepared for the transformation of *A. thaliana*. The promoter of *A. thaliana* plastidial pyruvate kinase β subunit gene (Pl-PK β 1, AT5G52920)[110][111] was used for the construction of ProPl-PK β 1: Px-sGFP by an LR reaction between *att*L1-ProPl-PK β 1-*att*L2 entry clone[111] and pGWB468.

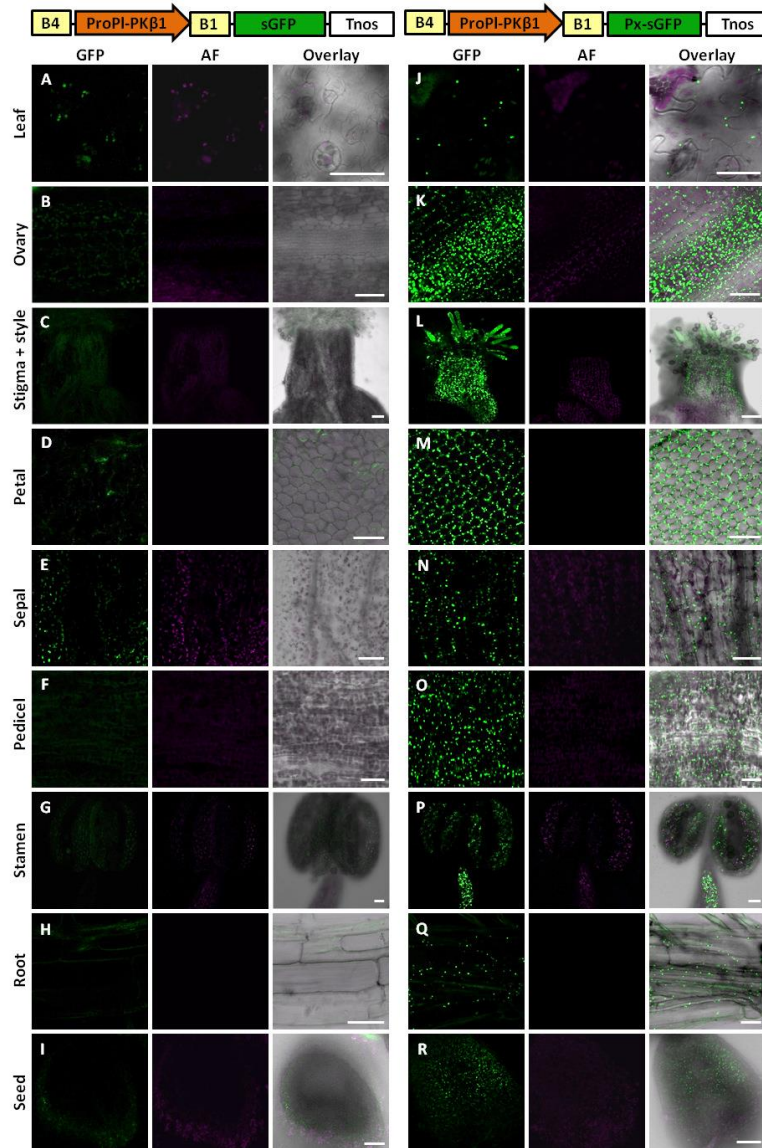


Fig. 2.3. Expression of sGFP and Px-sGFP driven by PI-PK β 1 promoter in transgenic *A. thaliana*. (A–I) images of ProPI-PK β 1:sGFP. (J–R) images of ProPI-PK β 1:Px-sGFP. (A and J) leaf, (B and K) ovary, (C and L) stigma + style, (D and M) petal, (E and N) sepal, (F and O) pedicel, (G and P) stamen, (H and Q) root, (I and R) seed. AF, autofluorescence; Overlay, overlay of GFP, AF, and differential interference contrast (DIC). Scale bars = 10 μ m.

The promoter and coding region of the gene for *A. thaliana* MYB21 (AT3G27810) were used for the construction of ProMYB21:MYB21-NLS-sGFP and ProMYB21:MYB21-Px-sGFP by LR reactions between *attL1*-ProMYB21:MYB21-*attL2* entry clone and pGWB565, or pGWB468, respectively. The promoter of the gene for *A.*

thaliana DAD1-LIKE LIPASE2 (DALL2, AT1G51440) was used for the construction of ProDALL2:NLS-sGFP by an LR reaction between *attL4*-ProDALL2-*attR1* entry clone and R4L1pGWB565. The promoter of the gene for *A. thaliana* 3-ketoacyl-CoA thiolase 2 (KAT2, AT2G33150) was used for the construction of ProKAT2:NLS-sGFP by an LR reaction between *attL4*-ProKAT2-*attR1* entry clone and R4L1pGWB565. We also prepared ProPI-PK β 1:sGFP, ProMYB21:MYB21-sGFP, ProDALL2:sGFP and ProKAT2:sGFP expressing sGFP without any organelle-targeting signals as reference constructs by LR reactions with corresponding entry clones and pGWB404 or R4L1pGWB504.

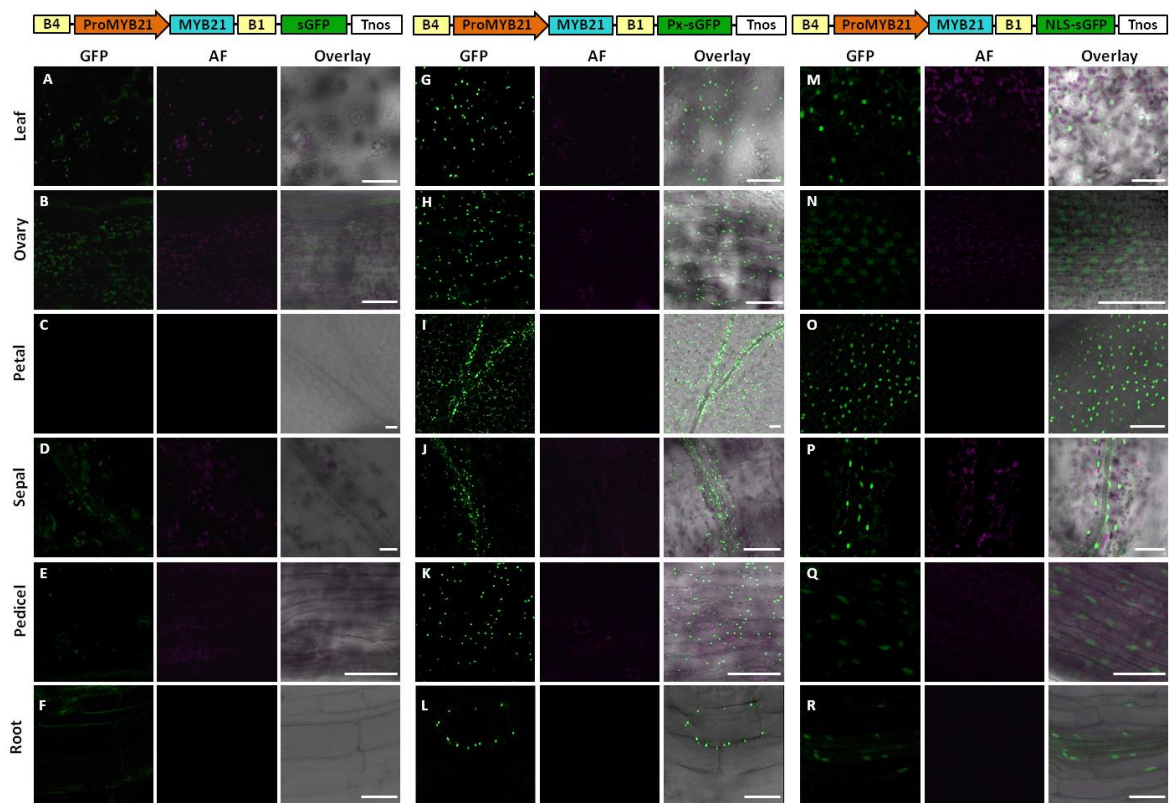


Fig. 2.4. Expression of MYB21-sGFP, MYB21-Px-sGFP and MYB21-NLS-sGFP driven by MYB21 promoter in transgenic *A. thaliana*. (A–F) images of ProMYB21:MYB21-sGFP. (G–L) images of ProMYB21:MYB21-Px-sGFP. (M–R) images of ProMYB21:MYB21-NLS-sGFP. (A, G, M) leaf, (B, H, N) ovary, (C, I, O) petal, (D, J, P) sepal, (E, K, Q) pedicel, (F, L, R) root. AF, autofluorescence; Overlay, overlay of GFP, AF, and DIC. Scale bars = 10 μ m.

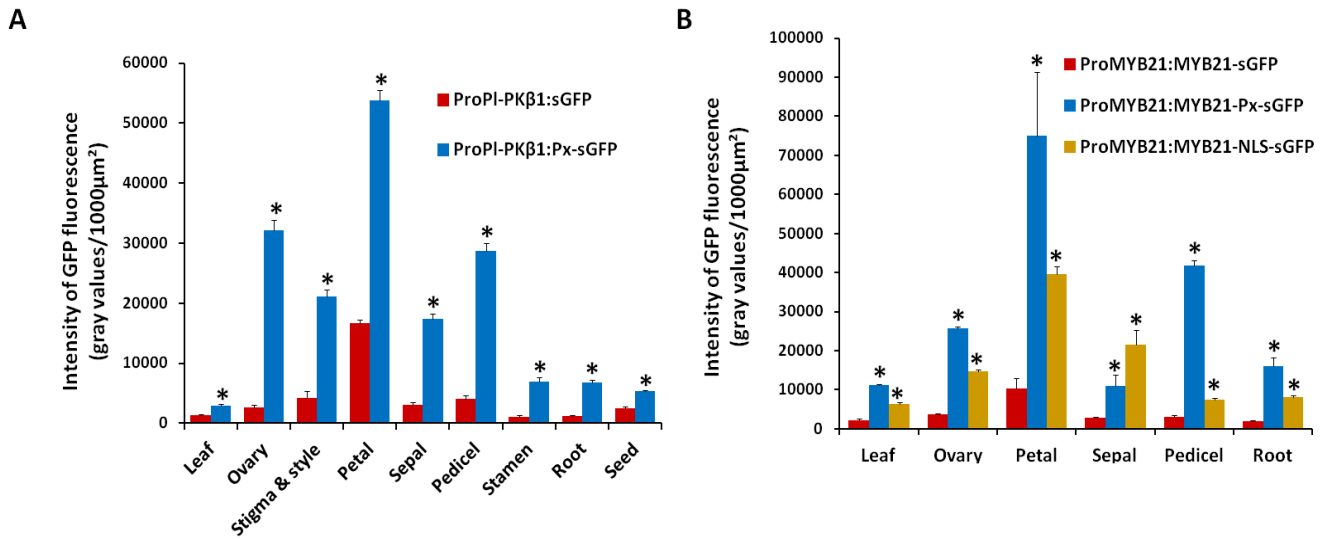


Fig. 2.5. Comparison of fluorescence intensities of sGFP and organelle-targeted sGFP among organs in transgenic *A. thaliana*. (A) Fluorescence intensities of ProPIPKβ1:sGFP and ProPI-PKβ1:Px-sGFP in various organs. (B) Fluorescence intensities of ProMYB21:MYB21-sGFP, ProMYB21:MYB21-Px-sGFP and ProMYB21:MYB21-NLS-sGFP in various organs. Error bars represent SD. * $p < 0.01$, Student's t-test.

These constructs were introduced into *A. thaliana* and selected transgenic *A. thaliana* were used for confocal microscopic analysis.

The plastidial pyruvate kinase catalyzes the transphosphorylation of phosphoenolpyruvate and ADP to pyruvate and ATP [112], and controlling the supply of pyruvate and ATP for fatty acid synthesis in the plastids. In *A. thaliana*, PI-PKβ1, a subunit of plastidial pyruvate kinase was shown to be expressed in the flower by promoter:GUS analysis [110]. In this study, we analyzed promoter activity by ProPI-PKβ1:sGFP and ProPI-PKβ1:Px-sGFP constructs. Because the *attL1*-ProPI-PKβ1-*attL2* entry clone carries -300 to +6 (A of initiation codon is +1) region, translation initiated from the entry clone in the binary constructs and the 13 amino acids MAHPAFLYKWDNS (third to thirteenth amino acids are derived from *attB2* site) was added to the N-terminal of sGFP and Px-sGFP. In ProPI-PKβ1:sGFP transgenic *A. thaliana*, a faint GFP fluorescence was observed only in stigma (Fig. 2.3A–I). In contrast, bright peroxisome-localized GFP fluorescence was observed in ovary, stigma, style, petal, sepal, pedicel, stamen, and maturing seeds of ProPI-PKβ1:Px-sGFP transgenic *A. thaliana* (Fig. 2.3K–P, R). The results obtained by Px-sGFP were consistent with previous reports using promoter:GUS [110][111]. We also

found weak expression in leaf and root (Fig. 2.3J and Q). In addition, we performed quantitative analysis and found a significant increase of fluorescence intensities in ProPl-PK β 1:Px-sGFP compared to ProPl-PK β 1:sGFP for all organs examined (Fig. 2.5A). These results indicated that promoter activity was monitored by Px-sGFP more sensitively than sGFP by accumulating expressed fluorescent protein in peroxisomes.

The *A. thaliana* MYB21 encodes an R2R3 MYB transcription factor controlling the development of petal, stamen, and carpel by stimuli of jasmonic acid. In a histochemical expression analysis of MYB21, promoter and entire coding region was used for a GUS fusion construct (ProMYB21:MYB21-GUS) and GUS activity was observed in filaments, style, and the vascular system of sepals and petals [105]. In this study, we analyzed expression of MYB21 by ProMYB21:MYB21-sGFP, ProMYB21:MYB21-Px-sGFP and ProMYB21:MYB21-NLS-sGFP constructs. We observed little or no GFP fluorescence in all examined organs of ProMYB21:MYB21-sGFP transgenic *A. thaliana* (Fig. 2.4A–F). In ProMYB21:MYB21-Px-sGFP transgenic *A. thaliana*, GFP fluorescence was clearly observed in the ovary and the vascular system of petals and sepals (Fig. 2.4H–J) as reported in [105]. We also observed strong expression in leaf, pedicel, and root (Fig. 2.4G, K, L). The GFP signals detected in these organs showed typical peroxisome-localization pattern as observed in Fig. 2.2B and 2.3, indicating that MYB21-Px-sGFP fusion protein was correctly accumulated in peroxisomes. In the Pro-MYB21:MYB21-NLS-sGFP transgenic *A. thaliana*, nucleus-localized GFP signal was observed in leaf, ovary, the vascular system of sepals and petals, pedicel, and root (Fig. 2.4M–R). The fluorescence intensities of ProMYB21:MYB21-Px-sGFP and ProMYB21:MYB21-NLS-sGFP were significantly increased compared to that of ProMYB21:MYB21-sGFP in all observed organs (Fig. 2.5B). These results showed the advantage of both Px-sGFP and NLS-sGFP for the detection of promoter activity and indicated the availability of entry clones including promoter and coding regions for highly sensitive expression analysis using fusion with PxsGFP or NLS-sGFP. Next, we examined expression by inducible promoters under noninduced conditions. *A. thaliana* DALL2 is a homolog of DAD1 with an expression known to be induced by wounding [109]. We prepared ProDALL2:sGFP and ProDALL2-NLS-sGFP using an *attL4*-Pro-DALL2-*attR1* entry clone with no initiation codon and analyzed their expressions in *A. thaliana*. In the leaves of ProDALL2:sGFP transgenic *A. thaliana*, we observed almost no GFP signals under non-induced conditions (Fig. 2.6A), and found only faint GFP fluorescence after wounding (Fig. 2.6B and I). On the other hand, nucleus-localized GFP signals were detected in leaves

of ProDALL2:NLS-sGFP transgenic *A. thaliana* even under non-induced conditions (Fig. 2.6C), with clear increasing of the frequency and intensity of GFP fluorescence after wounding (Fig. 2.6D, I). We also tested the promoter of *A. thaliana* KAT2, one of 3-ketoacyl-CoA thiolase. KAT2 catalyzes the final step of β -oxidation in peroxisomes for fatty acid metabolism and jasmonic acid production and its expression was found to be increased by dark-induced senescence in leaves [113][114]. We used the *attL4*-ProKAT2-*attR1* entry clone carrying -2074 to +6 region for preparation of ProKAT2:sGFP and ProKAT2:NLS-sGFP constructs. Therefore, sGFP and NLS-sGFP having the additional 12 amino acids METSLYKKAGSS (third to twelfth amino acids are derived from the *attB1* site) at the N-terminal were translated in this experiment. In leaves of ProKAT2:sGFP transgenic *A. thaliana*, we observed almost no GFP fluorescence under non-induced conditions (Fig. 2.6E) and a weak GFP fluorescence after dark treatment (Fig. 2.6F, J). In contrast, clear nucleus localized GFP fluorescence was observed in leaves of ProKAT2:NLSsGFP transgenic *A. thaliana* even under non-induced conditions (Fig. 2.6G) and the intensity and frequency of nucleus-localized GFP signals were drastically increased after dark treatment (Fig. 2.6H, J).

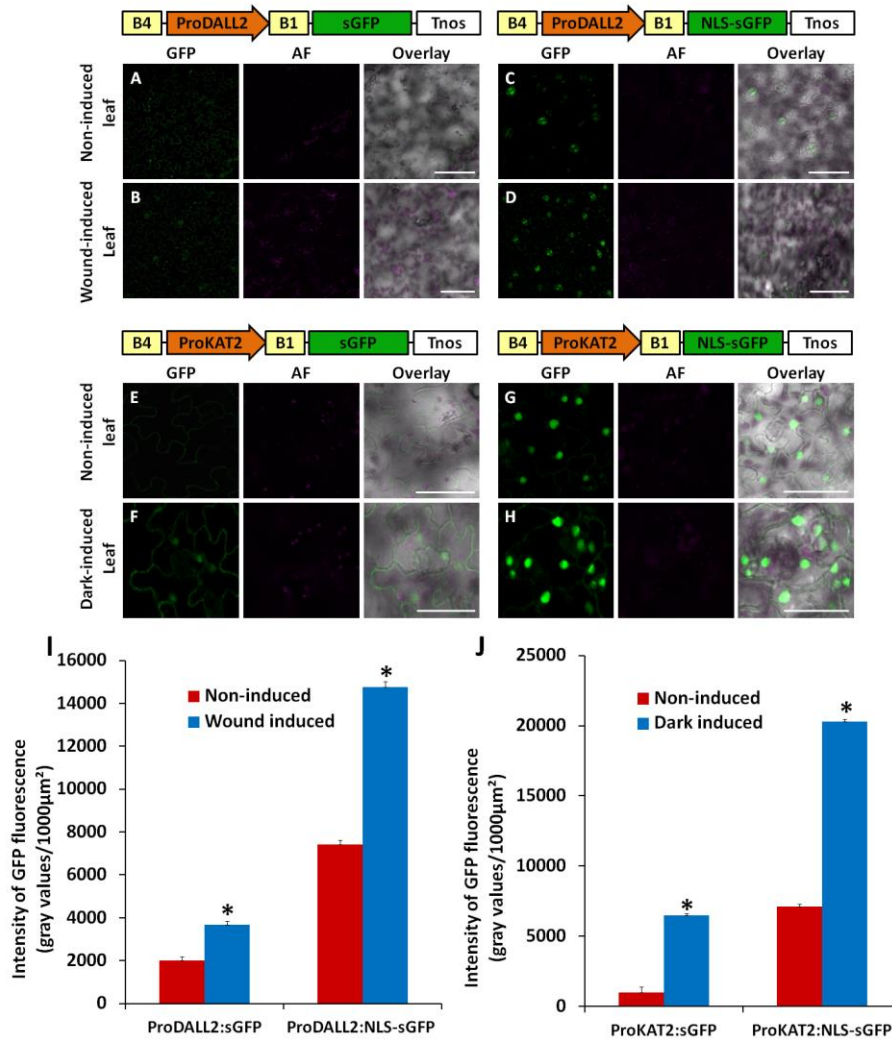


Fig. 2.6. Expression and comparison of fluorescence intensities of sGFP and NLS-sGFP driven by DALL2 and KAT2 promoters in transgenic *A. thaliana*. (A and B) images of ProDALL2:sGFP. (C and D) images of ProDALL2:NLS-sGFP. (A and C) non-induced condition, (B and D) 150 min after wounding. (E and F) images of ProKAT2:sGFP. (G and H) images of ProKAT2:NLS-sGFP. (E and G) non-induced condition, (F and H) 2 h after dark. (I) Fluorescence intensities in leaves of ProDALL2:sGFP and ProDALL2:NLS-sGFP after wound treatment. (J) Fluorescence intensities in leaves of ProKAT2:sGFP and ProKAT2:NLS-sGFP after dark treatment. AF, autofluorescence; Overlay, overlay of GFP, AF, and DIC. Scale bars = 10 μm . Error bars represent SD. * $p < 0.01$, Student's t-test.

These results indicated that visualization of a weak promoter activity under non-induced conditions was possible by organelle-targeted GFP equipped in the vector system described here. The organelle-targeted GFP also enhanced the intensity of fluorescence

signals under induced conditions and made possible the clear observation of gene expression.

In this study, we reported the construction and validity of the Gateway cloning technology-compatible binary vectors equipped with organelle-targeted fluorescent proteins for promoter assay in plants. Several localization targets are available in this system, including ER (ER-sGFP), nucleus (NLS-sGFP and NLS-TagRFP), peroxisome (Px-sGFP and Px-TagRFP), and mitochondria (Mt-sGFP and Mt-TagRFP). The binary vectors developed here are consisting of four selection-marker series (Km^r, Hyg^r, BASTA^r, and Tunica^r) to match a wide range of plant transformation experiments. Promoter entry clones of *attL1*-promoter-*attL2* and *attL4*-promoter-*attR1* types are available for preparation of promoter:organelle-targeted fluorescent protein constructs by LR reaction with developed pGWBs (*attR1-attR2* acceptor sites) and

R4L1pGWBs (*attR4-attL1* acceptor sites), respectively. We detected brighter fluorescence by the promoter:Px-sGFP and promoter:NLS-sGFP constructs than by the promoter:sGFP construct in transgenic *A. thaliana*. The vector system developed here has the advantage of high sensitivity in promoter:reporter assays by accumulating fluorescent proteins in target organelles.

Chapter 3

Expression analysis of genes encoding malectin-like domain (MLD)- and leucine4-rich repeat (LRR)- containing proteins in *Arabidopsis thaliana*

Malectin is a maltose- and related oligosaccharide binding protein in the endoplasmic reticulum that was initially identified in *Xenopus laevis*. It is widely conserved in animals and has been suggested to play a role in N-glycosylation of proteins[73]. In plants, for example in *A. thaliana*, the malectin-like domain (MLD) was found in the extracellular region of 17 receptor-like kinases (RLKs) belonging to the *Catharanthus roseus* RLK1-like (CrRLK1L) family and presumed to be a sensor for cell wall integrity [82][115]. At present, 10 of them have been analyzed for a variety of biological functions. FERONIA controls pollen tube function and vegetative cell growth[79][116]. ANXUR1 and ANXUR2 redundantly regulate cell wall integrity of pollen tubes[117]. THESEUS1 regulates cell growth during deficiency of cellulose synthesis and is thought to be a cell-wall-integrity sensor[118]. BUPS1 and BUPS2 play roles in tip growth of pollen tubes[119]. CURVY1 functions primarily in morphogenesis of trichomes and pavement cells[120]. ERULUS/CAP1 controls pollen tube growth and NH₄⁺ homeostasis-regulated root hair growth[121][122]. HERCULES1 and HERCULES2 regulate cell elongation in vegetative growth[123][124]. MLD was also found in IOS1, a different RLK from the CrRLK1L family, and contributed to pattern-triggered immunity[125]. In this study, we searched MLD-containing *A. thaliana* proteins other than RLK on InterPro (<http://www.ebi.ac.uk/interpro/>) to further analyze MLD and identified four proteins. These proteins contained leucine-rich repeat (LRR) in addition to MLD and were named AtMLLR1 (AT1G25570), AtMLLR2 (AT1G28340), AtMLLR3 (AT3G05990), and AtMLLR4 (AT3G19230). AtMLLR2 was previously identified as AtRLP4 in a genome-wide analysis of receptor-like proteins[126][126]. In this study, we used the designation of AtMLLR2 for AT1G28340. Fig. 3.1 shows the phylogenetic tree, domain structure and multiple alignments of AtMLLRs and MLD-containing RLKs. AtMLLR1 and 2 were predicted to be membrane-localizing receptor-like proteins composed of signal peptide (SP), MLD, LRR, and transmembrane domain (TMD). AtMLLR3 and 4 were predicted to be extracellular proteins composed of SP, MLD, and LRR. A phylogenetic analysis showed that all AtMLLRs were clustered in the same clade including IOS1 which carried MLD and LRR but were separated from the CrRLK1L family (Fig. 3.1A). These results indicate that AtMLLR1/2 initially branched from IOS1 through the loss of the kinase domain (KD), and AtMLLR3/4 then branched from IOS1 via the loss of TMD-KD. The amino acid identity of MLD between AtMLLR1 and

AtMLLR2 was 32.0%, while that between AtMLLR3 and AtMLLR4 was 43.1% (Fig. 3.1B).

To clarify the physiological functions of AtMLLRs, we initially examined the expression of AtMLLR2 and AtMLLR3 in detail using a promoter:GFP+promoter: GUS assay. The promoter entry clones pDONR201- ProAtMLLR2 carrying -1,997 to +3 of AtMLLR2 and pDONR201-ProAtMLLR3 carrying -2,142 to +3 of AtMLLR3 were prepared as described previously[95] with primers listed in Table 3.1.

Table 3.1. Synthetic Oligonucleotides

Oligos	Sequence
ProAtMLLR2-F	AAAAAGCAGGCTCCGACACTGCTAATGCTTTAAATGATGAAGG
ProAtMLLR2-R	AGAAAGCTGGGTAGACACTCATTGATTGATTTTTCTAGAAAGAA
ProAtMLLR3-F	AAAAAGCAGGCTCCGACACTACGAGCCAAGCGCAATGCT
ProAtMLLR3-R	AGAAAGCTGGGTAGACACTCATGGCGGCGGAGACGAC

To construct promoter: G3GFP+promoter:GUS using an *attL1*-promoter-*attL2* entry clone, we made pGWB3450 and pDD333, vectors of the dual-promoter:reporter Gateway cloning system, as follows. The *attR1-ccdB-attR2-G3GFP* fragment of pUGW50- Δ C[127] was introduced into pUGW3001 [127], and the resultant *attR1-ccdB-attR2-G3GFP-Tnos-Cm^r-attR4-ccdB-attR3* was introduced into pGWB400[95] to make pGWB3450. *ccdB*, *Cm^r*, and *Tnos* are a negative selection marker in *E. coli*, a chloramphenicol resistance marker, and nopaline synthase terminator, respectively. The *attL3-Tnos-attL4* fragment of L4L3pDD500[127] was introduced into pUC119 (TAKARA BIO, Otsu, Japan) to make pDD300. The *attR1-Cm^r-ccdB-attR2-GUS* fragment of pGWB433[95] was introduced into pDD300 to make pDD333. Fig. 3.2 shows the structures of pGWB3450 and pDD333 and an outline for the preparation of the dual-promoter:reporter binary construct ProAtMLLR:G3GFP+ProAtMLLR: GUS.

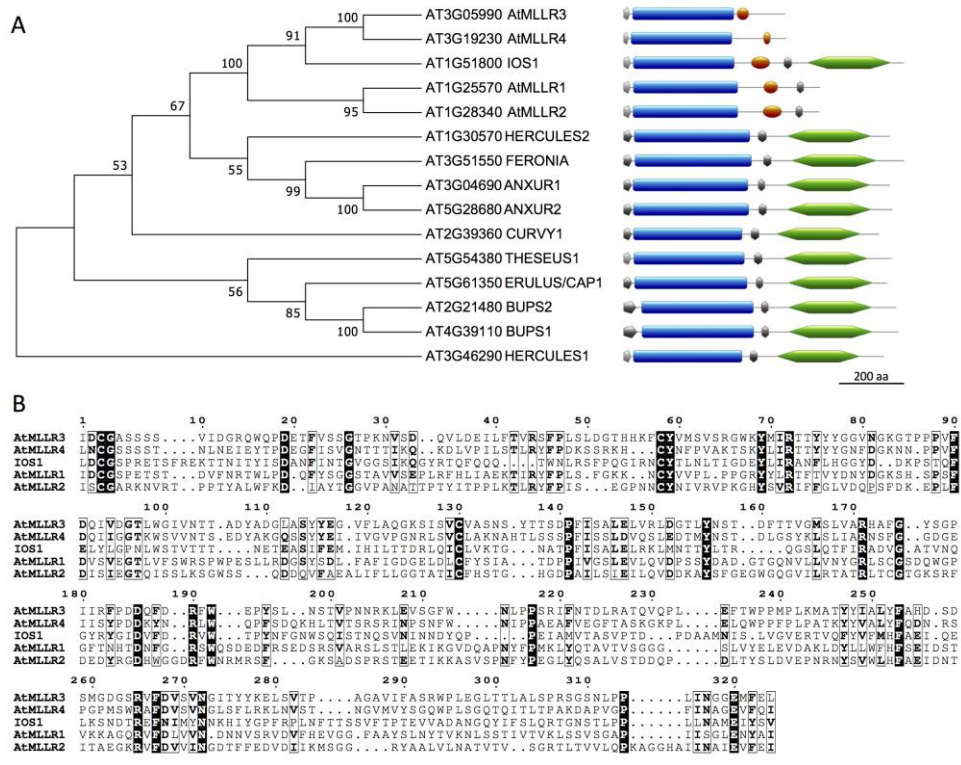


Fig. 3.1. Phylogenetic tree, domain structure and multiple alignments of AtMLLRs and MLD-containing RLKs in *A. thaliana*. (a) Left, Phylogenetic tree of the MLD for AtMLLRs and MLD-containing RLKs. Multiple alignments were performed with MUSCLE (<https://www.ebi.ac.uk/Tools/msa/muscle/>) and the phylogenetic tree was reconstructed with MEGA7 (www.megasoftware.net). Protein sequences are F4ICJ5 (AT1G25570, AtMLLR1), F4HWL3 (AT1G28340, AtMLLR2), Q9SFG3 (AT3G05990, AtMLLR3), F4JB46 (At3G19230, AtMLLR4), Q9C8I6 (AT1G51800, IOS1), Q9SR05 (AT3G04690, ANXUR1), Q3E8W4 (AT5G28680, ANXUR2), Q9T020 (AT4G39110, BUPS1), Q9SJT0 (AT2G21480, BUPS2), O80623 (AT2G39360, CURVY1), Q9FLJ8 (AT5G61350, ERULUS/CAP1), Q9SCZ4 (AT3G51550, FERONIA), Q9LX66 (AT3G46290, HERCULES1), Q9SA72 (AT1G30570, HERCULES2), and Q9LK35 (AT5G54380, THESEUS1). Right, Domain structure. Domains were predicted with Pfam (<http://pfam.xfam.org/>) and drawn by MyDomains (<http://prosite.expasy.org/mydomains/>). The predicted domains were shown as follows: pentagon (gray), SP; rectangle (blue), MLD; oval (red), LRR; vertical hexagon (gray), TMD; and horizontal hexagon (green), KD. (b) Multiple alignments of the MLD. The result of multiple alignments was presented with ESPrnt3.0 (<http://esprnt.ibcp.fr/ESPrnt/ESPrnt/>) for AtMLLR1-4 and IOS1. Highly conserved

residues were shown in bold text and boxed in black; strictly conserved residues were shown in black background.

The promoter entry clone pDONR201-ProAtMLLR2 was subjected to LR reactions with pDD333 and pGWB3450 according to Aboulela et al. 2017[127] for the construction of pGWB3450-ProAtMLLR2: G3GFP+ProAtMLLR2:GUS. pGWB3450-ProAtMLLR3: G3GFP+ProAtMLLR3:GUS was constructed in the same manner using pDONR201-ProAtMLLR3. A ProAtMLLR2:NLS-sGFP binary construct was prepared by an LR reaction with pDONR201-ProAtMLLR2 and pGWB565[110]. These constructs were used for transformation of *A. thaliana* as described previously[110]. Regarding GUS, seedlings (1, 4, 8, and 14-days after germination (DAG)) and dissected organs (40-DAG) from T3 lines of each construct were observed as described previously[128]. Fluorescence signals were examined as described previously[110]. Fig. 3.3 shows GUS staining and GFP fluorescence of transgenic *A. thaliana*. Regarding AtMLLR2, GUS staining was observed in the cotyledons, hypocotyl, and root of seedlings (Fig. 3.3A-E). In grown plants, we found the specific expression of GUS in guard cells, trichomes (Fig. 3.3F and J), pollen (Fig. 3.3G and H), and seeds (Fig. 3.3I). The expression of GFP was also detected in the trichome (Fig. 3.3K). We used the ProAtMLLR2:NLS-sGFP construct to increase the fluorescence signal [11] and, thus, easily detected bright GFP fluorescence in the nuclei of the trichome (Fig. 3.3L) and guard cells (Fig. 3.3M). Regarding AtMLLR3, GUS staining was observed in the root vascular bundle and root apical meristem of seedling (Fig. 3.3N-R). In grown plants, the vein (Fig. 3.3S), vascular bundle of the stem (Fig. 3.3 T and W), and trichome of young leaves (Fig. 3.3S) were stained. We also noted the expression of GUS at a very specific region in the flower, namely, the junction between the filament and anther (Fig. 3.3U and X). GFP fluorescence was observed in the root apical meristem (Fig. 3.3Y).

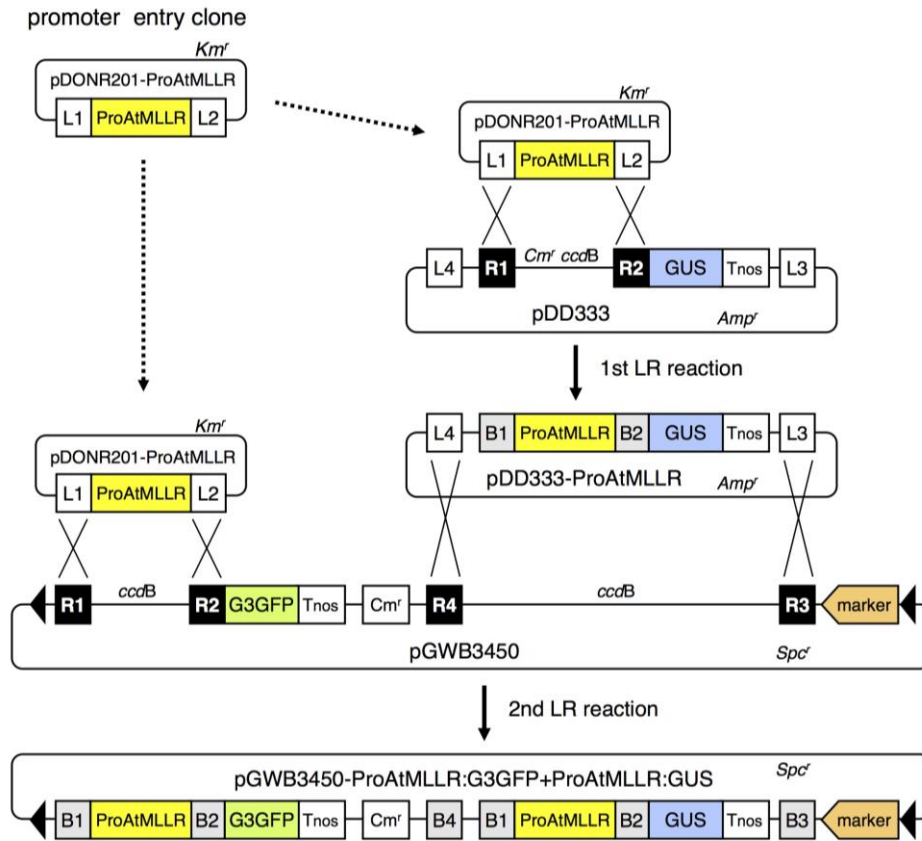


Fig. 3.2. Outline for the preparation of a ProAtMLLR:G3GFP+ProAtMLLR:GUS construct with pGWB3450 and pDD333. In the 1st LR reaction, ProAtMLLR in the promoter entry clone was transferred into pDD333 to make pDD333-ProAtMLLR. In the 2nd LR reaction, ProAtMLLR in the promoter entry clone and ProAtMLLR:GUS in pDD333-ProAtMLLR were transferred simultaneously into pGWB3450 to make pGWB3450-ProAtMLLR:G3GFP+ProAtMLLR:GUS.

Expression patterns in organs and cells shown by ProAtMLLR: reporter was consistent with information from the Arabidopsis eFP Browser (<http://bar.utoronto.ca/efp/cgi-bin/efpWeb.cgi>). GUS staining revealed the expression of AtMLLR3 at the junction between the filament and anther, the pattern of which was not displayed in the Arabidopsis eFP Browser possibly due to the difficulties associated with the accurate preparation of tissue. AtMLLR3 will be a unique marker gene that specifies the tissue connecting the filament and anther. The organs and cells expressing AtMLLRs in the present study will be good targets to search for and analyze phenotypes in corresponding T-DNA insertion lines. Since no phenotype was observed in the T-DNA

insertion line of AtRLP4 (AtMLLR2) [8], the double disruption of *AtMLLR2* and *AtMLLR1* may be needed to identify phenotypes for functional analyses. We found significant co-expression of *AtMLLR1* and 2 in an *in-silico* analysis with ATTED-II (<http://atted.jp>), supporting the possibility of redundancy in their physiological functions.

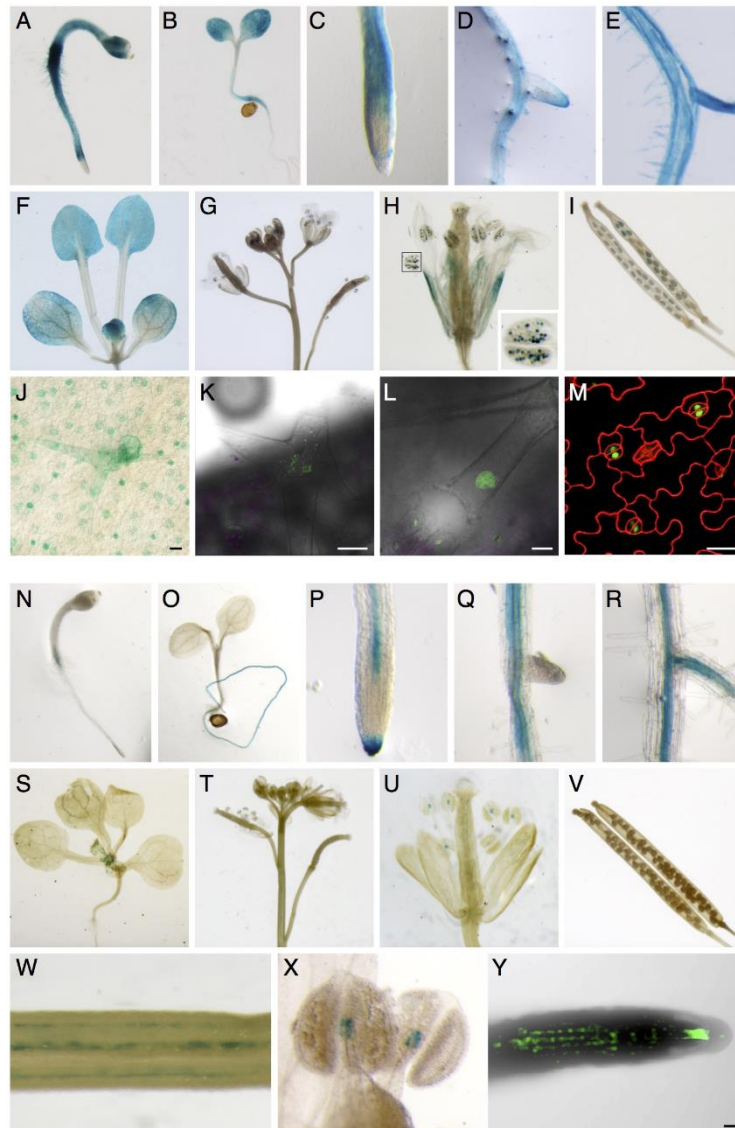


Fig. 3.3. Expression patterns of *AtMLLR* genes in *A. thaliana*. (A-K) ProAtMLLR2:G3GFP+ProAtMLLR2:GUS transgenic *A. thaliana*. GUS staining of 1-DAG seedling (A), 4-DAG seedling (B), 8-DAG roots (C-E), 14-DAG leaves (F), 40-DAG flowers and fruits (G-I). The inset shows magnified image of boxed anther (H). GUS staining of the trichome and guard cells (J). GFP fluorescence in the trichome (K). (L and M) ProAtMLLR2:NLS-sGFP transgenic *A. thaliana*. GFP fluorescence in the trichome (L). Merged image of GFP (green) and propidium iodide (red) in the leaf epidermis (M).

(N-Y) ProAtMLLR3:G3GFP+ProAtMLLR3:GUS transgenic *A. thaliana*. GUS staining of 1-DAG seedling (N), 4-DAG seedling (O), 8-DAG roots (P-R), 14-DAG leaves (S), 40-DAG flowers and fruits (T-V). GUS staining of the stem (W), and the junction between the filament and anther (X). GFP fluorescence in the root (Y). Bars = 20 μ m.

In conclusion, we identified four genes encoding MLD- and LRR-containing proteins in *A. thaliana*: two were predicted to be receptor-like proteins (AtMLLR1 and 2) and the other two were predicted to be extracellular proteins (AtMLLR3 and 4). The promoter:reporter assay on *AtMLLR2* and *3* showed the expression patterns of these genes, including the expression of *AtMLLR3* at the junction between the filament and anther. We developed a dual-promoter:reporter Gateway cloning system enabling promoter:GFP and promoter:GUS assays in one transgenic plant established by one transformation. This new system will be a useful tool and accelerate gene expression analyses of plants.

Chapter 4

Proposed conclusions

The author proposes the conclusions of this thesis as follows:

(i) The constructed Gateway binary vectors are useful for emitting high background fluorescence in subcellular localization analysis.

The author successfully developed a new series of Gateway cloning technology-compatible binary vectors, pGWBs (*attR1-attR2* acceptor sites) and R4L1pGWB (*attR4-attL1* acceptor sites). These vectors carry organelle-targeted synthetic green fluorescent protein (sGFP) (ER-, nucleus-, peroxisome-, and mitochondria-targeted sGFP) and organelle-targeted tag red fluorescent protein (TagRFP) (nucleus-, peroxisome-, and mitochondria-targeted TagRFP). The constructions accumulate fluorescent proteins in specific organelles, increases local brightness, enhanced the intensity of fluorescence signals in tissues emitting a high background of fluorescence that are advantageous in the bioscience field especially in subcellular localization analysis.

(ii) The constructed vectors serve as useful platform to facilitate promoter:reporter assay in plant.

The vector system developed by the author has promoter entry clones of *attL1*-promoter-*attL2* and *attL4*-promoter-*attR1* types are available for preparation of promoter:organelle-targeted fluorescent protein constructs by LR reaction to facilitate promoter:reporter assay (*attB1*-promoter-*attB2*-reporter and *attB4*-promoter-*attB1*-reporter) in plant. The advantages of high sensitivity promoter:reporter assays are to define organ-, tissue-, or cell-specific expression pattern of genes in detail and detect brighter fluorescence in transgenic *A. thaliana*.

(iii) The developed vector systems are valuable tools in the research field for expression analysis of genes

The new pGWBs and R4L1pGWBs developed by the author are highly efficient for observation of GFP and RFP signals in gene expression analyses of plants. The newly constructed vectors have the intracellular localization of organelle-targeted sGFP and TagRFPs, are effective and valuable tools in plant research. The developed vector systems also perform highly sensitive detection of promoter:organelle-targeted-sGFP or

promoter:cDNA-organelle-targeted-sGFP gene expression, prepared for the transformation of *A. thaliana*.

(iv) Identified genes support the possibility of their physiological functions.

The author identified four genes that encode malectin-like domain (MLD)- and leucine-rich repeat (LRR)-containing proteins (AtMLLRs): two were receptor-like proteins (AtMLLR1 and 2) and the other two were extracellular proteins (AtMLLR3 and 4) in *A. thaliana*. The expression patterns of these genes, including the expression of AtMLLR3 at the junction between the filament and anther suggested the involvement of many different physiological processes ranging from plant reproduction, cell elongation and growth by controlling unknown signaling events.

(v) Dual-site gateway cloning system benefits for comparison of expression patterns of genes.

The author used a dual-promoter:reporter gateway cloning system enabling promoter:GFP and promoter:GUS assays in one transgenic plant established by one transformation. The promoter: G3GFP+promoter: GUS assay indicated the organ- and cell-specific expression of the AtMLLR2 and AtMLLR3 genes, is very effective system that accelerate gene expression analyses of plants.

References

References

- [1] U. Krämer, “Planting molecular functions in an ecological context with *Arabidopsis thaliana*,” *Elife*, vol. 4, pp. 1–13, 2015.
- [2] O. Hedberg, “Afroalpine vascular plants : a taxonomic revision,” *Acta Universitatis Upsaliensis*, 1957.
- [3] A. Fulgione and A. M. Hancock, “Archaic lineages broaden our view on the history of *Arabidopsis thaliana*,” *New Phytol.*, vol. 219, no. 4, pp. 1194–1198, 2018.
- [4] M. Exposito-Alonso *et al.*, “The rate and potential relevance of new mutations in a colonizing plant lineage,” *PLoS Genet.*, vol. 14, no. 2, pp. 1–21, 2018.
- [5] H. Tsukaya, “Leaf development.,” *Arab. B.*, vol. 11, p. e0163, 2013.
- [6] S. Turner and L. E. Sieburth, “Vascular Patterning,” *Arab. B.*, vol. 2, p. e0073, 2003.
- [7] M. F. Yanofsky, H. Ma, J. L. Bowman, G. N. Drews, K. A. Feldmann, and E. M. Meyerowitz, “The protein encoded by the *Arabidopsis* homeotic gene *agamous* resembles transcription factors,” *Nature*, vol. 346, no. 6279, pp. 35–39, 1990.
- [8] D. W. Meinke, J. M. Cherry, C. Dean, S. D. Rounsley, and M. Koornneef, “*Arabidopsis thaliana*: A model plant for genome analysis,” *Science (80-.)*, vol. 282, no. 5389, 1998.
- [9] E. M. Meyerowitz, “*Arabidopsis*, a useful weed,” *Cell*, vol. 56, no. 2, pp. 263–269, 1989.
- [10] E. M. Meyerowitz and R. E. Pruitt, “Meyerowitz1985,” vol. 427, no. 1983, 1985.
- [11] N. J. Provart *et al.*, “50 years of *Arabidopsis* research: Highlights and future directions,” *New Phytol.*, vol. 209, no. 3, pp. 921–944, 2016.
- [12] S. J. Clough and A. F. Bent, “Floral dip: A simplified method for *Agrobacterium*-mediated transformation of *Arabidopsis thaliana*,” *Plant J.*, vol. 16, no. 6, pp. 735–743, 1998.
- [13] X. Zhang, R. Henriques, S. S. Lin, Q. W. Niu, and N. H. Chua, “*Agrobacterium*-mediated transformation of *Arabidopsis thaliana* using the floral dip method,” *Nat. Protoc.*, vol. 1, no. 2, pp. 641–646, 2006.
- [14] T. M. A. Magliano, J. F. Botto, A. V. Godoy, V. V. Symonds, A. M. Lloyd, and J.

- J. Casal, “New Arabidopsis recombinant inbred lines (Landsberg erecta x Nossen) reveal natural variation in phytochrome-mediated responses,” *Plant Physiol.*, vol. 138, no. 2, pp. 1126–1135, 2005.
- [15] A. Landy, “rights reserved DYNi \ MIC , STRUCTURAL , AND SITE-SPECIFIC RECOMBINATION,” *Annu. Rev. Biochem.*, vol. 58, pp. 913–949, 1989.
- [16] F. Katzen, “Gateway ® recombinational cloning: a biological operating system,” *Expert Opin. Drug Discov.*, vol. 2, no. 4, pp. 571–589, Apr. 2007.
- [17] 2† Albertha J. M. Walhout, 1* Raffaella Sordella, 1 Xiaowei Lu and 4 Marc Vidal | James L. Hartley, 3 Gary F. Temple, 3 Michael A. Brasch, 3 Nicolas Thierry-Mieg, 1, “Protein interaction mapping in *C. elegans* Using proteins involved in vulval development,” *Science (80-.)*, vol. 287, no. 5450, pp. 116–122, 2000.
- [18] Y. Tanaka *et al.*, “Gateway Vectors for Plant Genetic Engineering: Overview of Plant Vectors, Application for Bimolecular Fluorescence Complementation (BiFC) and Multigene Construction,” *Genet. Eng. - Basics, New Appl. Responsib.*, 2012.
- [19] S. De Folter *et al.*, “Comprehensive interaction map of the Arabidopsis MADS box transcription factors,” *Plant Cell*, vol. 17, no. 5, pp. 1424–1433, 2005.
- [20] J. L. Hartley, G. F. Temple, and M. A. Brasch, “SITE-SPECIFIC-RECOMBINATION-HARTLEY.pdf,” pp. 1788–1795, 2000.
- [21] A. Fontes, R. Quintanilla, and U. Lakshmi pathy, “Novel Platforms to Create Labeled Stem Cells,” in *Stem Cells in Clinic and Research*, InTech, 2011.
- [22] M. Karimi, A. Depicker, and P. Hilson, “Recombinational cloning with plant gateway vectors,” *Plant Physiol.*, vol. 145, no. 4, pp. 1144–1154, 2007.
- [23] M. D. Curtis and U. Grossniklaus, “A Gateway Cloning Vector Set for High-Throughput Functional Analysis of Genes in Planta,” *Plant Physiol.*, vol. 133, no. 2, pp. 462–469, 2003.
- [24] P. John and F. R. Whatley, “*Paracoccus denitrificans* and the evolutionary origin of the mitochondrion,” *Nature*, vol. 254, no. 5500, pp. 495–498, Apr. 1975.
- [25] R. J. Keenan, D. M. Freymann, R. M. Stroud, and P. Walter, “T s r p,” 2001.
- [26] T. Cavalier-Smith, “Membrane heredity and early chloroplast evolution,” *Trends Plant Sci.*, vol. 5, no. 4, pp. 174–182, 2000.

- [27] D. H. Kim and I. Hwang, "Direct Targeting of Proteins from the Cytosol to Organelles: The ER versus Endosymbiotic Organelles," *Traffic*, vol. 14, no. 6, pp. 613–621, 2013.
- [28] K. Kapp, M. K. Lemberg, and B. Dobberstein, "Post - Targeting Functions of Signal Peptides," no. April 2015, 2000.
- [29] G. Blobel and B. Dobberstein, "TRANSFER OF PROTEINS ACROSS MEMBRANES I. Presence of Proteolytically Processed and Unprocessed Nascent Immunoglobulin Light Chains On Membrane-Bound Ribosomes of Murine Myeloma GONTER," *J. Cell Biol.*, vol. 67, pp. 835–851, 1975.
- [30] R. S. Ullers, P. Genevoux, and J. Luirink, *Cotranslational Protein Targeting in Escherichia coli*, vol. 25, no. C. Elsevier Masson SAS, 2007.
- [31] P. Walter, I. Ibrahimi, and G. Blobel, "Translocation of proteins across the endoplasmic reticulum. I. Signal recognition protein (SRP) binds to in-vitro-assembled polysomes synthesizing secretory protein," *J. Cell Biol.*, vol. 91, no. 2 I, pp. 545–550, 1981.
- [32] J. Luirink and I. Sinning, "SRP-mediated protein targeting: Structure and function revisited," *Biochim. Biophys. Acta - Mol. Cell Res.*, vol. 1694, no. 1-3 SPEC.ISS., pp. 17–35, 2004.
- [33] A. K. J. Veenendaal, C. Van Der Does, and A. J. M. Driessen, "The protein-conducting channel SecYEG," *Biochim. Biophys. Acta - Mol. Cell Res.*, vol. 1694, no. 1-3 SPEC.ISS., pp. 81–95, 2004.
- [34] E. Hood, C. Cramer, G. Medrano, and J. Xu, "Protein targeting," in *Plant Biotechnology and Agriculture*, Elsevier, 2012, pp. 35–54.
- [35] M. Capitani and M. Sallese, "The KDEL receptor: New functions for an old protein," *FEBS Lett.*, vol. 583, no. 23, pp. 3863–3871, 2009.
- [36] K. G. Hardwick, M. J. Lewis, J. Semenza, N. Dean, and H. R. Pelham, "ERD1, a yeast gene required for the retention of luminal endoplasmic reticulum proteins, affects glycoprotein processing in the Golgi apparatus.," *EMBO J.*, vol. 9, no. 3, pp. 623–630, 1990.
- [37] J. C. Semenza, K. G. Hardwick, N. Dean, and H. R. B. Pelham, "ERD2, a yeast gene required for the receptor-mediated retrieval of luminal ER proteins from the

- secretory pathway,” *Cell*, vol. 61, no. 7, pp. 1349–1357, 1990.
- [38] H. R. Pelham, K. G. Hardwick, and M. J. Lewis, “Sorting of soluble ER proteins in yeast,” *EMBO J.*, vol. 7, no. 6, pp. 1757–1762, 1988.
- [39] E. C. Gaynor, S. Te Heesen, T. R. Graham, M. Aebi, and S. D. Emr, “Signal-mediated retrieval of a membrane protein from the Golgi to the ER in yeast,” *J. Cell Biol.*, vol. 127, no. 3, pp. 653–665, 1994.
- [40] M. R. Jackson, T. Nilsson, and P. A. Peterson, “Identification of a consensus motif for retention of transmembrane proteins in the endoplasmic reticulum,” *EMBO J.*, vol. 9, no. 10, pp. 3153–3162, 1990.
- [41] S. Munro and H. R. B. Pelham, “A C-terminal signal prevents secretion of luminal ER proteins,” *Cell*, vol. 48, no. 5, pp. 899–907, 1987.
- [42] H. R. Pelham, “Evidence that luminal ER proteins are sorted from secreted proteins in a post-ER compartment,” *EMBO J.*, vol. 7, no. 4, pp. 913–918, 1988.
- [43] K. Ishikawa *et al.*, “Dual targeting of a virus movement protein to ER and plasma membrane subdomains is essential for plasmodesmata localization,” *PLoS Pathog.*, vol. 13, no. 6, pp. 1–24, 2017.
- [44] D. Kalderon, B. L. Roberts, W. D. Richardson, and A. E. Smith, “A short amino acid sequence able to specify nuclear location,” *Cell*, vol. 39, no. 3 PART 2, pp. 499–509, 1984.
- [45] J. Robbins, S. M. Dilworth, R. A. Laskey, and C. Dingwall, “Two interdependent basic domains in nucleoplasmin nuclear targeting sequence: Identification of a class of bipartite nuclear targeting sequence,” *Cell*, vol. 64, no. 3, pp. 615–623, Feb. 1991.
- [46] C. Dingwall, J. Robbins, S. M. Dilworth, B. Roberts, and W. D. Richardson, “The nucleoplasmin nuclear location sequence is larger and more complex than that of SV-40 large T antigen,” *J. Cell Biol.*, vol. 107, no. 3, pp. 841–849, 1988.
- [47] M. T. Harreman, P. E. Cohen, M. R. Hodel, G. J. Truscott, A. H. Corbett, and A. E. Hodel, “Characterization of the auto-inhibitory sequence within the N-terminal domain of importin α ,” *J. Biol. Chem.*, vol. 278, no. 24, pp. 21361–21369, 2003.
- [48] D. Görlich, F. Vogel, A. D. Mills, E. Hartmann, and R. A. Laskey, “Distinct functions for the two importin subunits in nuclear protein import,” *Nature*, vol. 377,

no. 6546, pp. 246–248, Sep. 1995.

- [49] A. Lange, R. E. Mills, C. J. Lange, M. Stewart, S. E. Devine, and A. H. Corbett, “Classical Nuclear Localization Signals: Definition, Function, and Interaction with Importin α ,” *J. Biol. Chem.*, vol. 282, no. 8, pp. 5101–5105, Feb. 2007.
- [50] D. GORLICH, “Isolation of a protein that is essential for the first step of nuclear protein import,” *Cell*, vol. 79, no. 5, pp. 767–778, Dec. 1994.
- [51] D. Gilchrist, B. Mykytka, and M. Rexach, “Accelerating the rate of disassembly of karyopherin-cargo complexes,” *J. Biol. Chem.*, vol. 277, no. 20, pp. 18161–18172, 2002.
- [52] T. Kanazawa *et al.*, “SNARE molecules in *Marchantia polymorpha*: Unique and conserved features of the membrane fusion machinery,” *Plant Cell Physiol.*, vol. 57, no. 2, pp. 307–324, 2016.
- [53] S. J. Gould, G. A. Keller, and S. Subramani, “Identification of a peroxisomal targeting signal at the carboxy terminus of firefly luciferase,” *J. Cell Biol.*, vol. 105, no. 6 II, pp. 2923–2931, 1987.
- [54] P. B. Lazarow and Y. Fujiki, “Biogenesis of peroxisomes,” *Annu. Rev. Cell Biol.*, vol. 1, pp. 489–530, 1985.
- [55] V. Dammai and S. Subramani, “The human peroxisomal targeting signal receptor, Pex5p, is translocated into the peroxisomal matrix and recycled to the cytosol,” *Cell*, vol. 105, no. 2, pp. 187–196, 2001.
- [56] B. W. Swinkels, S. J. Gould, A. G. Bodnar, R. A. Rachubinski, and S. Subramani, “A novel, cleavable peroxisomal targeting signal at the amino-terminus of the rat 3-ketoacyl-coA thiolase,” *Trends Cell Biol.*, vol. 10, no. 11, pp. 3255–3262, 1991.
- [57] J. R. Glover, D. W. Andrews, S. Subramani, and R. A. Rachubinski, “Mutagenesis of the amino targeting signal of *Saccharomyces cerevisiae* 3-ketoacyl-CoA thiolase reveals conserved amino acids required for import into peroxisomes in vivo,” *J. Biol. Chem.*, vol. 269, no. 10, pp. 7558–7563, 1994.
- [58] I. Van der Leij, M. M. Franse, Y. Elgersma, B. Distel, and H. F. Tabak, “PAS10 is a tetratricopeptide-repeat protein that is essential for the import of most matrix proteins into peroxisomes of *Saccharomyces cerevisiae*,” *Proc. Natl. Acad. Sci. U. S. A.*, vol. 90, no. 24, pp. 11782–11786, 1993.

- [59] H. Wimmer, H. Mayringer, and K. Landerl, "Poor Reading: A Deficit in Skill-Automatization or a Phonological Deficit?," *Sci. Stud. Read.*, vol. 2, no. 4, pp. 321–340, Oct. 1998.
- [60] A. J. Urquhart, D. Kennedy, S. J. Gould, and D. I. Crane, "Interaction of Pex5p, the type 1 peroxisome targeting signal receptor, with the peroxisomal membrane proteins Pex14p and Pex13p," *J. Biol. Chem.*, vol. 275, no. 6, pp. 4127–4136, 2000.
- [61] S. Reumann, "Specification of the peroxisome targeting signals type 1 and type 2 of plant peroxisomes by bioinformatics analyses," *Plant Physiol.*, vol. 135, no. 2, pp. 783–800, 2004.
- [62] M. Marzioch, R. Erdmann, M. Veenhuis, and W. H. Kunau, "PAS7 encodes a novel yeast member of the WD-40 protein family essential for import of 3-oxoacyl-CoA thiolase, a PTS2-containing protein, into peroxisomes.," *EMBO J.*, vol. 13, no. 20, pp. 4908–4918, 1994.
- [63] P. Rehling, M. Marzioch, F. Niesen, E. Wittke, M. Veenhuis, and W. H. Kunau, "The import receptor for the peroxisomal targeting signal 2 (PTS2) in *Saccharomyces cerevisiae* is encoded by the PAS7 gene.," *EMBO J.*, vol. 15, no. 12, pp. 2901–2913, 1996.
- [64] G. Blobel, "Intracellular protein topogenesis (protein translocation across membranes/protein integration into membranes/posttranslocational sorting/topogenic sequences/ phylogeny of membranes and compartments)," *Cell Biol.*, vol. 77, no. 3, pp. 1496–1500, 1980.
- [65] G. Schatz and B. Dobberstein, "Common Principles of Protein Translocation Across Membranes," *Science (80-.)*, vol. 271, no. 5255, pp. 1519–1526, Mar. 1996.
- [66] G. von Heijne, "A new method for predicting signal sequence cleavage sites," *Nucleic Acids Res.*, vol. 14, no. 11, pp. 4683–4690, 1986.
- [67] D. Rapaport, "Finding the right organelle. Targeting signals in mitochondrial outer-membrane proteins," *EMBO Rep.*, vol. 4, no. 10, pp. 948–952, 2003.
- [68] J. Huang *et al.*, "RAD18 transmits DNA damage signalling to elicit homologous recombination repair," *Nat. Cell Biol.*, vol. 11, no. 5, pp. 592–603, May 2009.
- [69] M. Maduke and D. Roise, "Structure and function of mitochondrial presequences,"

1996, pp. 49–79.

- [70] Y. Abe *et al.*, “Structural basis of presequence recognition by the mitochondrial protein import receptor Tom20,” *Cell*, vol. 100, no. 5, pp. 551–560, 2000.
- [71] N. Pfanner, “Protein sorting: Recognizing mitochondrial presequences,” *Curr. Biol.*, vol. 10, no. 11, pp. R412–R415, Jun. 2000.
- [72] M. F. Bauer, S. Hofmann, W. Neupert, and M. Brunner, “Protein translocation into mitochondria: The role of TIM complexes,” *Trends Cell Biol.*, vol. 10, no. 1, pp. 25–31, 2000.
- [73] T. Schallus *et al.*, “Malectin: A Novel Carbohydrate-binding Protein of the Endoplasmic Reticulum and a Candidate Player in the Early Steps of Protein N - Glycosylation,” *Mol. Biol. Cell*, vol. 19, no. 8, pp. 3404–3414, Aug. 2008.
- [74] S. Moussu, S. Augustin, A. O. Roman, C. Broyart, and J. Santiago, “Crystal structures of two tandem malectin-like receptor kinases involved in plant reproduction,” *Acta Crystallogr. Sect. D Struct. Biol.*, vol. 74, no. 7, pp. 671–680, 2018.
- [75] L. Lehle, S. Strahl, and W. Tanner, “Protein glycosylation, conserved from yeast to man: A model organism helps elucidate congenital human diseases,” *Angew. Chemie - Int. Ed.*, vol. 45, no. 41, pp. 6802–6818, 2006.
- [76] P. Deprez, M. Gautschi, and A. Helenius, “More than one glycan is needed for ER glucosidase II to allow entry of glycoproteins into the calnexin/calreticulin cycle,” *Mol. Cell*, vol. 19, no. 2, pp. 183–195, 2005.
- [77] T. Schallus, K. Fehér, U. Sternberg, V. Rybin, and C. Muhle-Goll, “Analysis of the specific interactions between the lectin domain of malectin and diglucosides,” *Glycobiology*, vol. 20, no. 8, pp. 1010–1020, 2010.
- [78] S. J. Galli, N. Borregaard, and T. A. Wynn, “Phenotypic and functional plasticity of cells of innate immunity: macrophages, mast cells and neutrophils,” *Nat. Immunol.*, vol. 12, no. 11, pp. 1035–1044, Nov. 2011.
- [79] J.-M. Escobar-Restrepo *et al.*, “The FERONIA Receptor-like Kinase Mediates Male-Female Interactions During Pollen Tube Reception,” *Science (80-.)*, vol. 317, no. 5838, pp. 656–660, Aug. 2007.
- [80] S. Galindo-Trigo, J. E. Gray, and L. M. Smith, “Conserved roles of CrRLK1L

- receptor-like kinases in cell expansion and reproduction from algae to angiosperms,” *Front. Plant Sci.*, vol. 7, no. AUG2016, pp. 1–10, 2016.
- [81] S. Du, L. J. Qu, and J. Xiao, “Crystal structures of the extracellular domains of the CrRLK1L receptor-like kinases ANXUR1 and ANXUR2,” *Protein Sci.*, vol. 27, no. 4, pp. 886–892, 2018.
- [82] C. M. Franck, J. Westermann, and A. Boisson-Dernier, “Plant Malectin-Like Receptor Kinases: From Cell Wall Integrity to Immunity and Beyond,” *Annu. Rev. Plant Biol.*, vol. 69, no. 1, 2018.
- [83] G. Jedd and N. H. Chua, “Visualization of peroxisomes in living plant cells reveals acto-myosin-dependent cytoplasmic streaming and peroxisome budding,” *Plant Cell Physiol.*, vol. 43, no. 4, pp. 384–392, 2002.
- [84] S. Mano, C. Nakamori, M. Hayashi, A. Kato, M. Kondo, and M. Nishimura, “Distribution and characterization of peroxisomes in Arabidopsis by visualization with GFP: Dynamic morphology and actin-dependent movement,” *Plant Cell Physiol.*, vol. 43, no. 3, pp. 331–341, 2002.
- [85] Y. Lo, L. Hsiao, W. Jane, Y. Charng, H. Dai, and K. Chiang, “GFP-Targeted Mitochondria Show Heterogeneity of Size, Morphology, and Dynamics in Transgenic *Nicotiana tabacum* L. Plants In Vivo,” *Int. J. Plant Sci.*, vol. 165, no. 6, pp. 949–955, Nov. 2004.
- [86] D. C. Logan and C. J. Leaver, “Mitochondria-targeted GFP highlights the heterogeneity of mitochondrial shape, size and movement within living plant cells,” *J. Exp. Bot.*, vol. 51, no. 346, pp. 865–871, 2000.
- [87] R. Matsushima, Y. Hayashi, M. Kondo, T. Shimada, M. Nishimura, and I. Hara-Nishimura, “An endoplasmic reticulum-derived structure that is induced under stress conditions in Arabidopsis,” *Plant Physiol.*, vol. 130, no. 4, pp. 1807–1814, 2002.
- [88] J. Dalal *et al.*, “A novel gateway-compatible binary vector series (PC-GW) for flexible cloning of multiple genes for genetic transformation of plants,” *Plasmid*, vol. 81, no. 8, pp. 55–62, Sep. 2015.
- [89] K. W. Earley *et al.*, “Gateway-compatible vectors for plant functional genomics and proteomics,” *Plant J.*, vol. 45, no. 4, pp. 616–629, 2006.

- [90] K. Ishizaki *et al.*, “Development of gateway binary vector series with four different selection markers for the liverwort *marchantia polymorpha*,” *PLoS One*, vol. 10, no. 9, pp. 1–13, 2015.
- [91] M. Karimi, D. Inzé, and A. Depicker, “Trends in Plant Science Volume 7 issue 5 2002 [doi 10.1016%2Fs1360-1385%2802%2902251-3] Mansour Karimi; Dirk Inzé; Ann Depicker -- GATEWAY™ vectors for Agrobacterium-mediated plant transformation.pdf,” vol. 7, no. 5, pp. 193–195, 2002.
- [92] C. Wang *et al.*, “A Series of TA-Based and Zero-Background Vectors for Plant Functional Genomics,” *PLoS One*, vol. 8, no. 3, pp. 1–10, 2013.
- [93] R. Zhong, C. Lee, J. Zhou, R. L. McCarthy, and Z. H. Ye, “A battery of transcription factors involved in the regulation of secondary cell wall biosynthesis in *Arabidopsis*,” *Plant Cell*, vol. 20, no. 10, pp. 2763–2782, 2008.
- [94] T. Nakagawa, S. Ishiguro, and T. Kimura, “Gateway vectors for plant transformation,” *Plant Biotechnol.*, vol. 26, no. 3, pp. 275–284, 2009.
- [95] T. Nakagawa *et al.*, “Improved gateway binary vectors: High-performance vectors for creation of fusion constructs in transgenic analysis of plants,” *Biosci. Biotechnol. Biochem.*, vol. 71, no. 8, pp. 2095–2100, 2007.
- [96] T. Nakagawa *et al.*, “Development of series of gateway binary vectors, pGWBs, for realizing efficient construction of fusion genes for plant transformation,” *J. Biosci. Bioeng.*, vol. 104, no. 1, pp. 34–41, 2007.
- [97] S. Nakamura *et al.*, “Gateway binary vectors with the bialaphos resistance gene, bar, as a selection marker for plant transformation,” *Biosci. Biotechnol. Biochem.*, vol. 74, no. 6, pp. 1315–1319, 2010.
- [98] Y. TANAKA, K. SHIBAHARA, and T. NAKAGAWA, “Development of Gateway Binary Vectors R4L1pGWB Possessing the Bialaphos Resistance Gene (bar) and the Tunicamycin Resistance Gene as Markers for Promoter Analysis in Plants,” *Biosci. Biotechnol. Biochem.*, vol. 77, no. 8, pp. 1795–1797, Aug. 2013.
- [99] S. Nakamura, A. Nakao, M. Kawamukai, T. Kimura, S. Ishiguro, and T. Nakagawa, “Development of Gateway binary vectors, R4L1pGWBs, for promoter analysis in higher plants,” *Biosci. Biotechnol. Biochem.*, vol. 73, no. 11, pp. 2556–2559, 2009.
- [100] Y. Tanaka, S. Nakamura, M. Kawamukai, N. Koizumi, and T. Nakagawa,

- “Development of a series of Gateway binary vectors possessing a tunicamycin resistance gene as a marker for the transformation of *Arabidopsis thaliana*,” *Biosci. Biotechnol. Biochem.*, vol. 75, no. 4, pp. 804–807, 2011.
- [101] M. cloning: a laboratory Manual. and T. Sambrook, J.; Fritsch, E. F.; Maniatis, *Exported Abstract record (s)*, vol. 1. 2001.
- [102] W. Chiu, Y. Niwa, W. Zeng, T. Hirano, H. Kobayashi, and J. Sheen, “<Chiu_1996_CurrBiol_Engineered GFP as a vital reporter in plants.pdf>,” pp. 325–330.
- [103] M. Takeuchi, T. Ueda, K. Sato, H. Abe, T. Nagata, and A. Nakano, “A dominant negative mutant of Sar1 GTPase inhibits protein transport from the endoplasmic reticulum to the Golgi apparatus in tobacco and *Arabidopsis* cultured cells,” *Plant J.*, vol. 23, no. 4, pp. 517–525, 2000.
- [104] S. Lee *et al.*, “Mitochondrial Targeting of the *Arabidopsis* F1-ATPase γ -Subunit via Multiple Compensatory and Synergistic Presequence Motifs,” *Plant Cell*, vol. 24, no. 12, pp. 5037–5057, Dec. 2012.
- [105] P. H. Reeves *et al.*, “A regulatory network for coordinated flower maturation,” *PLoS Genet.*, vol. 8, no. 2, 2012.
- [106] T. Hino, Y. Tanaka, M. Kawamukai, K. Nishimura, S. Mano, and T. Nakagawa, “Two Sec13p homologs, AtSec13A and AtSec13B, redundantly contribute to the formation of COPII transport vesicles in *Arabidopsis thaliana*,” *Biosci. Biotechnol. Biochem.*, vol. 75, no. 9, pp. 1848–1852, 2011.
- [107] D. Weigel and J. Glazebrook, “*Arabidopsis*: a laboratory manual,” p. 354, 2002.
- [108] M. Narusaka, T. Shiraishi, M. Iwabuchi, and Y. Narusaka, “The floral inoculating protocol: A simplified *Arabidopsis thaliana* transformation method modified from floral dipping,” *Plant Biotechnol.*, vol. 27, no. 4, pp. 349–351, 2010.
- [109] I. Ruduś *et al.*, “Wound-induced expression of DEFECTIVE IN ANTHET DEHISCENCE1 and DAD1-like lipase genes is mediated by both CORONATINE INSENSITIVE1-dependent and independent pathways in *Arabidopsis thaliana*,” *Plant Cell Rep.*, vol. 33, no. 6, pp. 849–860, 2014.
- [110] M. M. Sultana *et al.*, “Gateway binary vectors with organelle-targeted fluorescent proteins for highly sensitive reporter assay in gene expression analysis of plants,”

J. Biotechnol., vol. 297, no. 3, pp. 19–27, May 2019.

- [111] K. Maeo *et al.*, “An AP2-type transcription factor, WRINKLED1, of *Arabidopsis thaliana* binds to the AW-box sequence conserved among proximal upstream regions of genes involved in fatty acid synthesis,” *Plant J.*, vol. 60, no. 3, pp. 476–487, 2009.
- [112] G. Valentini, L. Chiarelli, R. Fortini, M. L. Speranza, A. Galizzi, and A. Mattevi, “The allosteric regulation of pyruvate kinase: A site-directed mutagenesis study,” *J. Biol. Chem.*, vol. 275, no. 24, pp. 18145–18152, 2000.
- [113] M. C. Castillo and J. León, “Expression of the β -oxidation gene 3-ketoacyl-CoA thiolase 2 (KAT2) is required for the timely onset of natural and dark-induced leaf senescence in *Arabidopsis*,” *J. Exp. Bot.*, vol. 59, no. 8, pp. 2171–2179, 2008.
- [114] M. C. Castillo, C. Martínez, A. Buchala, J. P. Métraux, and J. León, “Gene-specific involvement of β -oxidation in wound-activated responses in *Arabidopsis*,” *Plant Physiol.*, vol. 135, no. 1, pp. 85–94, 2004.
- [115] C. Li, H. Wu, and A. Y. Cheung, “FERONIA and her pals: functions and mechanisms,” *Plant Physiol.*, vol. 171, no. 4, p. pp.00667.2016, Jun. 2016.
- [116] Q. Duan, D. Kita, C. Li, A. Y. Cheung, and H. M. Wu, “FERONIA receptor-like kinase regulates RHO GTPase signaling of root hair development,” *Proc. Natl. Acad. Sci. U. S. A.*, vol. 107, no. 41, pp. 17821–17826, 2010.
- [117] A. Boisson-Dernier, D. S. Lituiev, A. Nestorova, C. M. Franck, S. Thirugnanarajah, and U. Grossniklaus, “ANXUR Receptor-Like Kinases Coordinate Cell Wall Integrity with Growth at the Pollen Tube Tip Via NADPH Oxidases,” *PLoS Biol.*, vol. 11, no. 11, 2013.
- [118] K. Hématy *et al.*, “A Receptor-like Kinase Mediates the Response of *Arabidopsis* Cells to the Inhibition of Cellulose Synthesis,” *Curr. Biol.*, vol. 17, no. 11, pp. 922–931, 2007.
- [119] L. Zhu, L. C. Chu, Y. Liang, X. Q. Zhang, L. Q. Chen, and D. Ye, “The *Arabidopsis* CrRLK1L protein kinases BUPS1 and BUPS2 are required for normal growth of pollen tubes in the pistil,” *Plant J.*, vol. 95, no. 3, pp. 474–486, 2018.
- [120] E. W. Gachomo, L. Jno Baptiste, T. Kefela, W. M. Saidel, and S. O. Kotchoni, “The *Arabidopsis* CURVY1 (CVY1) gene encoding a novel receptor-like protein kinase

- regulates cell morphogenesis, flowering time and seed production,” *BMC Plant Biol.*, vol. 14, no. 1, pp. 1–9, 2014.
- [121] S. Schoenaers, D. Balcerowicz, A. Costa, and K. Vissenberg, “The kinase ERULUS controls pollen tube targeting and growth in *Arabidopsis thaliana*,” *Front. Plant Sci.*, vol. 8, no. November, pp. 1–10, 2017.
- [122] L. Bai *et al.*, “A receptor-like kinase mediates ammonium homeostasis and is important for the polar growth of root hairs in *Arabidopsis*,” *Plant Cell*, vol. 26, no. 4, pp. 1497–1511, 2014.
- [123] H. Guo, L. Li, H. Ye, X. Yu, A. Algreen, and Y. Yin, “Three related receptor-like kinases are required for optimal cell elongation in *Arabidopsis thaliana*,” *Proc. Natl. Acad. Sci. U. S. A.*, vol. 106, no. 18, pp. 7648–7653, 2009.
- [124] H. Guo, H. Ye, L. Li, and Y. Yin, “Brassinosteroid regulated receptor-like kinases,” *Plant Signal. Behav. Signal. Behav.*, vol. 48, no. 4, pp. 784–786, 2009.
- [125] Y. H. Yeh *et al.*, “The arabidopsis malectin-like/LRR-RLK IOS1 is critical for BAK1-dependent and BAK1-independent pattern-triggered immunity,” *Plant Cell*, vol. 28, no. 7, pp. 1701–1721, 2016.
- [126] G. Wang *et al.*, “A genome-wide functional investigation into the roles of receptor-like proteins in arabidopsis,” *Plant Physiol.*, vol. 147, no. 2, pp. 503–517, 2008.
- [127] M. Aboulela *et al.*, “Development of an R4 dual-site (R4DS) gateway cloning system enabling the efficient simultaneous cloning of two desired sets of promoters and open reading frames in a binary vector for plant research,” *PLoS One*, vol. 12, no. 5, pp. 1–18, 2017.
- [128] S. Nakamura, T. Suzuki, M. Kawamukai, and T. Nakagawa, “Expression analysis of *Arabidopsis thaliana* small secreted protein genes,” *Biosci. Biotechnol. Biochem.*, vol. 76, no. 3, pp. 436–446, 2012.

List of publications

Chapter 2

Mst Momtaz Sultana, Amit Kumar Dutta, Yuji Tanaka, Mostafa Aboulela, Kohji Nishimura, Sayaka Sugiura, Tomoko Niwa, Kenichiro Maeo, Shino Goto-Yamada, Tetsuya Kimura, Sumie Ishiguro, Shoji Mano Tsuyoshi Nakagawa (2019) Gateway binary vectors with organelle-targeted fluorescent proteins for highly sensitive reporter assay in gene expression analysis of plants. *Journal of Biotechnology*, 297:19–27. (<https://doi.org/10.1016/j.jbiotec.2019.03.015>).

Chapter 3

Mst Momtaz Sultana, Takushi Hachiya, Amit Kumar Dutta, Kohji Nishimura, Takamasa Suzuki, Ai Tanaka & Tsuyoshi Nakagawa (2019) Expression analysis of genes encoding malectin-like domain (MLD)- and leucine-rich repeat (LRR)- containing proteins in *Arabidopsis thaliana*. *Bioscience, Biotechnology, and Biochemistry*, DOI:10.1080/09168451.2019.1661769.

Acknowledgements

Acknowledgements

First and foremost, I would like to express my deepest gratitude to **Prof. Dr. Tsuyoshi NAKAGAWA**, Director of the Center of Integrated Research in Science, Shimane University, for constant encouragement, support, and invaluable suggestions that made my work successful. During my tenure, he contributed to widen my experience by giving me intellectual freedom in my work and inspiring me with humble politeness to do my research. I would also like to thank him for the careful consideration to finish my research; without his genial and supportive efforts my degree would have undoubtedly been more difficult.

I want to convey my deepest gratitude to **Dr. HACHIYA TAKUSHI** (Shimane University), for providing me helpful suggestion and support, especially regarding my second paper.

I wish to express my sincere thanks to **Prof. Dr. Makoto KAWAMUKAI**, **Associate Prof. Dr. Tomohiro KAINO**, and **Assistant Prof. Dr. Yasuhiro MATSUO** (Shimane University), for providing me with invaluable advice and comments on my research in regular meetings and seminars throughout the course of this work.

I am very grateful to **Assistant Prof. Dr. Kohji NISHIMURA** (Shimane University), for the kind guidance and for the technical support especially concerning particle bombardment and confocal microscopy imaging.

I would also like to thank the rest of my thesis committee, **Associate Prof. Tomoya Esumi** (Shimane University), **Prof. Kinya AKASHI** (Tottori University) for their observant suggestions and for kind supervision.

I wish also to express my sincere thanks to **Prof. Tetsuya KIMURA**, (Mie University), **Associate Prof. Sumie ISHIGURO** (Nagoya University), and **Associate Prof. Shoji MANO**, (National Institute for Basic Biology), for the invaluable advice and their comments on the manuscripts.

My sincere thanks go to **Amit Dutta**, **Dr. Yuji TANAKA** and **Dr. Mostafa ABOULELA** for their crucial contribution and technical support; without their efforts my work would have undoubtedly been more difficult.

My heartiest thanks go to **Michael Nil N. Nartey** for the invaluable advice and help concerning real time PCR.

I would like to express my thanks to my present and past colleagues, **Toshiki SAISHO, Shoya YOKOYAMA, Aoi SHIBAHARA, Mihiko YAMAZAKI, Mayu KODANI, Md. Firose Hossain, Kana TAKEMURA** and **Saki Sanemoto** all members of the laboratory of Life Science and Biotechnology, for their cordial support and for being great friends throughout my stay in Japan.

Many thanks go to the Ministry of Education, Culture, Sports, Science and Technology of Japan (MEXT) for giving me this opportunity to study my Ph.D. degree at united graduate school of agricultural science and for the financial support.

Finally, I would like to express my heartfelt thanks to my family members for all their affection and inspiration. I want to convey my deepest gratitude to my beloved husband **Md Hafizur Rahman Hafiz**, my son **Jawaad Labeeb Mahi** and my lovely daughter **Juwayriyya Laibah Manha** for their crucial support, services and inspiration both in my lab. work and household work.

Summary

Summary

The research described in this thesis has a specific goal to develop gateway compatible binary vector construction and their strategies in detail for the study of organ-, tissue-, or cell-specific expression pattern of genes in *Arabidopsis thaliana* through promoter:reporter assay. In this section the results of the study are summarized below:

In **Chapter 1**, the author presents a general introduction to the work. **Chapter 2** describes development of new vectors and expression analysis of genes in *Arabidopsis thaliana*. A new series of Gateway cloning technology-compatible binary vectors, pGWBs (*attR1-attR2* acceptor sites) and R4L1pGWB (*attR4-attL1* acceptor sites), carrying organelle-targeted sGFP (ER-, nucleus-, peroxisome-, and mitochondria-targeted sGFP) and organelle-targeted TagRFP (nucleus-, peroxisome-, and mitochondria-targeted TagRFP) has been developed to facilitate promoter:reporter assays in *A. thaliana*. To confirm the intracellular localization of newly developed organelle-targeted TagRFP constructs, co-localization analysis by transient expression were done using Pro35S:NLS-sGFP (established nucleus localization marker), Pro35S:NLS-TagRFP, Pro35S:Px-sGFP (established peroxisome localization marker), Pro35S:Px-TagRFP, Pro35S:Mt-sGFP (established mitochondria localization marker), Pro35S:Mt-TagRFP constructs by particle bombardment into Japanese leek epidermal cells. Confocal microscopic analysis revealed the correct co-localization of newly constructed TagRFPs in plant cells. In order to analyze the performance of newly constructed vectors for highly sensitive detection of gene expression, ProPI-PK β 1:Px-sGFP for pGWB565 and ProMYB21:MYB21-NLS-sGFP and ProMYB21:MYB21-Px-sGFP for pGWB565, and pGWB468, respectively were used. ProPI-PK β 1:sGFP and ProMYB21:MYB21-sGFP constructs were used as control. Confocal microscopic results indicated that promoter activity was monitored more sensitively with organelle targeted sGFP than normal sGFP by accumulating expressed fluorescent protein in peroxisomes and nucleus. Expression of *A. thaliana* DALL2 and KAT2 increases when induced by wounding and dark respectively. Wound induction of ProDALL2:sGFP, ProDALL2:NLS-sGFP construct and dark induction of ProKAT2:sGFP, ProKAT2:NLS-sGFP constructs revealed that fluorescence signals of organelle-targeted GFP were enhanced and made possible clear observation of gene expression. NLS-sGFP was also detected under non-inducible conditions.

MLD was found in extracellular domain of some plant RLK and presumed to be a sensor of extracellular environment. In **Chapter 3** four new proteins of *A. thaliana* containing leucine-rich repeat (LRR) in addition to MLD were identified and were named AtMLLR1 (AT1G25570), AtMLLR2 (AT1G28340), AtMLLR3 (AT3G05990), and AtMLLR4 (AT3G19230). To understand physiological functions of these proteins, AtMLLR2 and AtMLLR3, were initially examined by expression analysis using a promoter:G3GFP+promoter:GUS (ProAtMLLR:G3GFP+ProAtMLLR:GUS) assay concerning AtMLLR2, GUS staining was observed in the cotyledons, hypocotyl, and root of seedlings, specifically in guard cells, trichomes, pollen, and seeds. Concerning AtMLLR3, GUS staining was observed in the root vascular bundle and root apical meristem of seedling, growing plants vein, vascular bundle of the stem, and trichome of young leaves and at a very specific region in the flower, namely, the junction between the filament and anther. The expression of GFP was observed in the trichome and root apical meristem of AtMLLR2 and AtMLLR3 respectively. The pGWB565 vector described in chapter 2 was also used to confirm specific expression and bright GFP fluorescence in the nuclei of the trichome and guard cells were detected from ProAtMLLR2:NLS-sGFP construct.

In the **Chapter 4**, the author provides proposed conclusion remarks and discusses the findings presented in this study.

Overall, total 56 of Gateway cloning technology-compatible binary vectors carrying organelle localization strategies described in this thesis, provides an effective approach to robustly enhance the expression, have been considered to meet the demands of fundamental research. For the first step toward understanding physiological function of *AtMLLR* gene, expression of *AtMLLR2* and 3 were analyzed in detail with dual-promoter:reporter Gateway cloning system and organelle targeting fluorescent protein. Moreover, *AtMLLR* genes provide an invaluable resource to the plant community, allowing for fast generation of a variety of tissue-specific GUS and GFP expression constructs. In conclusion, a set of Gateway-compatible vectors provide a reliable cloning method for organ-, tissue-, or cell-specific gene expression by quick formation of expression constructs will be a beneficial tool for many biological researches.

要旨

本論文は新たな Gateway クローニング対応バイナリベクターの開発と、プロモーター：レポーターアッセイによるシロイヌナズナ遺伝子の器官、組織、あるいは細胞特異的発現パターンの詳細な解析を目指したものである。以下のように要約する。

第1章では、本研究のイントロダクションを述べる。第2章では、新しいベクターの開発とシロイヌナズナ遺伝子発現解析について記す。プロモーター：レポーターによる遺伝子発現解析をより推進するため、オルガネラ標的蛍光タンパク質である小胞体標的 sGFP (ER-sGFP)、核標的 sGFP (NLS-sGFP)、ペルオキシソーム標的 sGFP (Px-sGFP)、ミトコンドリア標的 sGFP (Mt-sGFP)、核標的 TagRFP (NLS-TagRFP)、ペルオキシソーム標的 TagRFP (Px-TagRFP)、ミトコンドリア標的 TagRFP (Mt-TagRFP) を赤色蛍光タンパク質 (TagRFP) をそれぞれ搭載した新しい Gateway クローニング対応バイナリベクターの開発を行った。アクセプターサイトが *attR1-attR2* である pGWB と *attR4-attL1* である R4L1pGWB のシリーズが作られている。新たに構築したオルガネラ標的 TagRFP が正しい局在を示すことを確認するため、Pro35S:NLS-sGFP (核標的 sGFP マーカー) と Pro35S:NLS-TagRFP、Pro35S:Px-sGFP (ペルオキシソーム標的 sGFP マーカー) と Pro35S:Px-TagRFP、Pro35S:Mt-sGFP (ミトコンドリア標的 sGFP マーカー) と Pro35S:Mt-TagRFP を遺伝子銃にてネギ表皮細胞に撃ち込み、共局在解析を行った。共焦点レーザー顕微鏡観察により新規構築オルガネラ標的 TagRFP が正しい局在を示すことが明らかとなった。次に、遺伝子発現高感度検出の性能試験のため、pGWB565 を用いて ProPl-PKβ1:Px-sGFP、ProMYB21:MYB21-NLS-sGFP、pGWB468 を用いて ProMYB21:MYB21-Px-sGFP が構築され発現解析が行われた。コントロールとして、ProPl-PKβ1:sGFP と ProMYB21:MYB21-sGFP が使われた。共焦点レーザー顕微鏡観察の結果、通常の sGFP に比べて核やペルオキシソームに蓄積するオルガネラ標的 sGFP の方がはるかに高感度で遺伝子発現をモニターできることが明らかとなった。障害誘導性 DALL2 プロモーター、暗老化誘導性 KAT2 プロモーターについても NLS-

sGFPの方が通常の sGFP よりも発現誘導が明瞭に観察された。また、NLS-sGFP では非誘導条件下でも蛍光シグナルが観察された。

MLDは植物 RLK の細胞外ドメインに見出され、細胞外環境のセンサーとして働くと推測されている。第3章では、MLD と LRR を持つ新たなシロイヌナズナタンパク質遺伝子 4 種が同定され、AtMLLR1 (AT1G25570)、AtMLLR2 (AT1G28340)、AtMLLR3 (AT3G05990)および AtMLLR4 (AT3G19230)と名付けられた。これらタンパク質の生理機能を明らかにするため、新たに開発した dual-promoter:reporter Gateway cloning system を利用して AtMLLR2 と 3 の promoter:GFP+promoter:GUS 発現解析が行われた。AtMLLR2 の GUS 染色は子葉、胚軸、根で見られ、また孔辺細胞、トライコーム、花粉と種子でも観察された。AtMLLR3 の GUS 染色は芽生えにおいて根の維管束と根端分裂組織で見られ、成長した植物では葉脈、茎の維管束、若い葉のトライコームで観察された。花においては、葯と花糸の連結部という非常に限定された領域で GUS 染色が見られた。AtMLLR2 ではトライコームにおいて、AtMLLR3 では根端分裂組織において GFP 蛍光が観察された。AtMLLR2 の解析には第2章で開発した pGWB565 も用いられ、トライコームと孔辺細胞における核局在 sGFP シグナルが明瞭に観察された。

第4章では結論と考察を述べた。

本研究では、56 の Gateway クローニング対応オルガネラ標的蛍光タンパク質が開発された。AtMLLR 遺伝子の生理機能解明に向け、AtMLLR2 と 3 の発現解析が dual-promoter:reporter Gateway cloning system とオルガネラ標的蛍光タンパク質 pGWB で行われ、AtMLLR 遺伝子が特異部位での発現遺伝子として植物研究に有効であることも考えられた。本研究で開発されたベクターシステムでは迅速な遺伝子コンストラクションが可能であり、多くの研究者に有用な遺伝子発現ツールである。